Nuclear Energy Agency

NEA/CSNI/R(2020)14

Unclassified **English text only**

13 February 2023

NUCLEAR ENERGY AGENCY
COMMITTEE ON THE SAFETY OF NUCLEAR INSTALLATIONS

Cancels & replaces the same document of 2 December 2022

Behaviour of Iodine Project 3: Final Summary Report

This document is available in PDF format only.

JT03512218

COMMITTEE ON THE SAFETY OF NUCLEAR INSTALLATIONS

The Committee on the Safety of Nuclear Installations (CSNI) addresses Nuclear Energy Agency (NEA) programmes and activities that support maintaining and advancing the scientific and technical knowledge base of the safety of nuclear installations.

The Committee constitutes a forum for the exchange of technical information and for collaboration between organisations, which can contribute, from their respective backgrounds in research, development and engineering, to its activities. It has regard to the exchange of information between member countries and safety R&D programmes of various sizes in order to keep all member countries involved in and abreast of developments in technical safety matters.

The Committee reviews the state of knowledge on important topics of nuclear safety science and techniques and of safety assessments, and ensures that operating experience is appropriately accounted for in its activities. It initiates and conducts programmes identified by these reviews and assessments in order to confirm safety, overcome discrepancies, develop improvements and reach consensus on technical issues of common interest. It promotes the co-ordination of work in different member countries that serve to maintain and enhance competence in nuclear safety matters, including the establishment of joint undertakings (e.g. joint research and data projects), and assists in the feedback of the results to participating organisations. The Committee ensures that valuable end-products of the technical reviews and analyses are provided to members in a timely manner, and made publicly available when appropriate, to support broader nuclear safety.

The Committee focuses primarily on the safety aspects of existing power reactors, other nuclear installations and new power reactors; it also considers the safety implications of scientific and technical developments of future reactor technologies and designs. Further, the scope for the Committee includes human and organisational research activities and technical developments that affect nuclear safety.

Table of contents

List of figures

List of tables

List of abbreviations and acronyms

AECL	Atomic Energy of Canada Limited
ASTEC	A commercially-available severe accident analysis code (developed by IRSN, France)
AWG	Analytical Working Group
BIP	Behaviour of Iodine Project
CNL	Canadian Nuclear Laboratories (formerly AECL)
CNRA	Committee on Nuclear Regulatory Activities (NEA)
COCOSYS	A commercially-available severe accident analysis code (developed by GRS, Germany)
CRPPH	Committee on Radiological Protection and Public Health (NEA)
ECD	Electron Capture Detector
FID	Flame ionisation detector
GC	Gas chromatography
GRS	Gesellschaft für Anlagen- und Reaktorsicherheit (Germany)
INSPAIR	A mechanistic iodine chemistry research code (developed by NNL, United Kingdom)
IOx	Iodine oxides
IRSN	Institut de Radioprotection et de Sûreté Nucléaire (France)
JAEA	Japan Atomic Energy Agency
KICHE(OrgIDB)	A mechanistic iodine chemistry research code (developed by JAEA, Japan)
LIRIC	Library of iodine reactions in containment, a phenomenological research code (developed by AECL, now CNL, Canada)
MELCOR	A commercially-available severe accident code (developed by SNL, United States)
NEA	Nuclear Energy Agency
NNL	National Nuclear Laboratory (United Kingdom)
OECD	Organisation for Economic Co-operation and Development
ORGI	Organic iodide
PRG	Program review group
RH	Relative humidity

RWMC	Radioactive Waste Management Committee (NEA)
SNL	Sandia National Laboratories (United States)
STEM	Source term evaluation and mitigation project (IRSN, France)
TCD	Thermal conductivity detector
THAI	Thermal-hydraulics Hydrogen Aerosol Iodine project
TIC	Total inorganic carbon
TOC	Total organic carbon

Executive summary

The present report summarises the main results and learnings from the third phase of the Nuclear Energy Agency (NEA) Behaviour of Iodine Project (BIP-3), which was conducted between 2016 and 2019 by the Canadian Nuclear Laboratories (CNL).

An NEA state-of-the-art report on iodine chemistry published in February 2007 concluded that there were still several aspects of iodine behaviour in containment during severe accidents that warranted further investigation. Over the past 25 years, there have been several NEA initiatives and other programmes to enhance the understanding of iodine chemistry, including the Phébus FP and International Source Term Project, the NEA Thermal-hydraulics Hydrogen Aerosol Iodine (THAI) Projects, the NEA Source Term Evaluation and Mitigation (STEM) Projects and the NEA Behaviour of Iodine Projects (BIP).

BIP was created to investigate the interactions between iodine and paint. The adsorption of iodine onto epoxy paint and the subsequent radiolytic production and release of organic iodides from painted containment surfaces were topics of particular interest. A database of iodine deposition data was accumulated in BIP-1 and expanded in BIP-2, with experiments focused on improving mechanistic understanding of the nature of the iodine-paint interactions.

A third phase of BIP was initiated by the NEA in 2016, with Canadian Nuclear Laboratories (CNL)[1] as the operating agent. Topics for BIP-3 were chosen to leverage the CNL's existing facilities and expertise. The BIP-3 experimental programme was structured to address important and unresolved topics from the BIP-1 and BIP-2 programmes as well as knowledge gaps that arise when attempting to extrapolate results to postulated nuclear accident conditions. Additionally, collaborative analytical activities, co-ordinated through the BIP-3 Analytical Working Group (AWG), were completed as part of the NEA BIP-3 scope of work.

Although other parameters were also studied, BIP-3 mainly focused on the effects of different paint ageing strategies (natural, pre-irradiation, and thermal treatments) on iodine behaviour. Specifically, the effects of ageing on the quantity of releasable organic products from the paint, the iodine sorption behaviour, and the subsequent rate of radiolytic methyl iodide production were evaluated. Studies relating to radiolytic CH_3I production in the gas phase were also performed. Several experiments also expanded on previous themes and topics of interest in BIP-1 and BIP-2. The impact of pre-exposing painted coupons to reactive gases such as NO_2 and Cl_2 was studied using higher concentrations and longer exposure periods, and a final test was performed to evaluate the role of water in the organic iodide production mechanism. Finally, several scoping tests were performed to assist in the interpretation and modelling of BIP and STEM data, including tests to evaluate iodine behaviour with glass and O-ring surfaces, as well as tests exploring the sorption behaviour of iodine for a wide range of surface loading concentrations and as a function of the gaseous iodine loading concentration.

The NEA BIP-3 project was initiated in January 2016 with signatories from 11 member countries: Belgium, Canada, Finland, France, Germany, Japan, Korea, Sweden, Switzerland, the United Kingdom and the United States. The total project budget was established at EUR 1 million, half of which was contributed by Canada (CNL) as the operating agent. All project deliverables were originally intended to be completed by July 2019. However, a series of critical equipment failures in the last year of the project led to an extended schedule at no

1. Previously Atomic Energy of Canada Limited (AECL).

extra cost to the members; tests continued until the end of June 2019, and the associated analysis and documentation activities continued through March 2020.

Overall, the BIP-3 programme has continued to enrich the database of iodine kinetic data available for researchers and analysts in support of model development. Tests have affirmed that paint is an important sink for iodine in containment, and have provided significant insights into the role of paint ageing on iodine sorption and the production of organic iodide.

The iodine adsorption process was shown to depend on paint type, age, the presence of competing reactive species, loading temperature, relative humidity and the I_2 exposure concentration. Specifically:

- Slower deposition velocity was generally observed on paints with increased age (natural or simulated), and combined ageing strategies had a larger effect.
- Increased paint age is believed to contribute to enhanced surface modification (through chemical breakdown of components of the paint structure), such that the number of available active sites for iodine adsorption are reduced.
- Pre-exposures to reactive gases such as NO_2 and Cl_2 led to an induction period for iodine adsorption, and initial iodine deposition rates were among the lowest observed in BIP.
- Higher deposition velocities are observed under higher temperatures and relative humidities.
- Exposure to higher iodine loading concentrations leads to lower deposition velocities and higher relative iodine desorption.

Key conclusions with respect to methyl iodide production were as follows:

- Lower CH_3I production is observed for paint with increased ageing (natural or simulated), and the combination of ageing strategies leads to a greater reduction.
- Gas phase production of CH_3I from the reaction of I_2 and CH_4 appears to be very small.
- Other organic-based materials (O-ring) can contribute to CH_3I production, particularly over the long term.
- The CH_3I peak observed for aqueous loaded irradiation tests in BIP-1 and 2 experiments appears to be associated with the aqueous adsorption process rather than the simple presence of water in the paint matrix, and suggests the nature of the iodine-paint bond is different for gas and aqueous loaded tests.

Key conclusions from the AWG modelling exercises were as follows:

- All models predicted that the inclusion of organic iodide production from painted surfaces would increase the total airborne iodine for a postulated accident scenario, and similar overall trends were predicted for iodine behaviour and volatility with respect to sump acidification.
- Significant variations in general modelling capabilities and modelling strategies still exist. In particular, there was little consistency among the models in the selection of I_2 deposition velocity, or the treatment of mass transfer.
- There was also a lack of consensus on which chemical processes were considered, and the outcomes of those processes, such as consideration of the possible gas phase reaction of I_2 with volatile organic compounds or gas phase formation of iodine oxides (IOx) from the radiolysis of I_2 or organic iodides.

- Differences in the phenomenology considered among the codes (particularly in the gas phase) can strongly impact model predictions.

While BIP-3 experiments have shown that paint ageing can have a significant effect on iodine sorption and organic iodide production, the overall consequences of this phenomenon on predictions of iodine speciation and volatility should be assessed. The AWG modelling exercises also revealed that there are considerable differences in the iodine phenomenology considered and the treatment of key parameters in the different iodine-paint interaction models, and this can strongly impact the model predictions. This indicates that continued refinement of our understanding of fundamental iodine chemistry pathways is needed to ensure continued model development is based on accurate mechanistic behaviour. Additionally, continued model development efforts should endeavour to limit the potential for user effects to impact on model outcomes and, wherever possible, fitting parameters should be independent of the test considered.

Gaps still remain in the understanding of iodine-paint interactions that can impact predictions of iodine source term in containment. In particular, the relative importance of radiolytic gas phase reactions between I_2 and volatile organic compounds on methyl iodide production remains unclear. Resolution will require additional tests with an improved analytical method. Tests to assess the organic iodide production from organics in containment other than paint (e.g. cable coatings) could be considered in future research programmes to assist in model development and to better quantify predictions of iodine source term.

1. Introduction

The present report summarises the main results and learnings from the third phase of the Nuclear Energy Agency (NEA) Behaviour of Iodine Project (BIP-3), which was conducted between 2016 and 2019 by the Canadian Nuclear Laboratories (CNL) to address knowledge gaps on iodine behaviour in the containment of light water reactors during a severe accident. The focus of the experimental investigations was on iodine interaction with aged paints, the resulting iodine trapping by the containment painted surfaces and on organic iodides formation in the containment. Such investigations are of specific relevance for developing models for the calculation of radioactive iodine release to the environment in case of a severe accident.

2. BIP-3 project description

2.1. Overview

Continued improvement of existing computer models to predict post-accident fission product behaviour in containment relies on a comprehensive understanding of all relevant phenomena and high-confidence data. Unexpected iodine behaviour observed during the international Phébus FP programme highlighted the need for a greater understanding of iodine behaviour. This conclusion was further captured in an NEA state-of-the-art report on iodine chemistry published in February 2007 [1]. There have been several NEA initiatives to study the behaviour of iodine in containment including the THAI, STEM and BIP projects. The development of a computational model that can universally reproduce the experimental observations from each of these projects is the primary long-term goal. In support of this, experimental programmes such as BIP have focused on collecting quantitative data that are necessary inputs for iodine behaviour models (such as iodine deposition velocities onto various substrates) or that can be used to assist in model validation exercises, as well as qualitative data that can be used to guide model design and inform on plausible reaction pathways.

Although a few other containment surfaces have been tested, the BIP project has focused on iodine retention and subsequent release from epoxy paint, which is a commonly used coating within containment buildings throughout the world. Epoxy paint is a complex mixture of polymeric compounds, and the nature of iodine's interaction with this surface is not fully understood. The BIP projects have endeavoured to resolve some of these uncertainties. In BIP-1, experiments investigating the role of water on the deposition velocities and formation of methyl iodide from irradiated paint showed that adsorbed water strongly affected both the sorption and organic iodide formation processes [2]. While BIP- 2 investigated the same processes, emphasis was placed on developing a more detailed mechanistic understanding of the iodine-paint interactions [3]. Experiments using various polymeric compounds as model compounds for different structures within the paint demonstrated that the iodine adsorption and radiolytically-driven organic iodide formation are not limited to a single functional group on the paint. Many parts of the paint structure will participate in these processes, although some structures are more important (e.g. the amide groups). The first experiments to study the effect of other gases within containment such as NO_2 (formed by air radiolysis) or Cl_2 (formed by degradation of cable insulation) on the iodine-paint interaction were also performed in BIP-2, although no effect was observed at the relatively low concentrations studied.

In BIP-1 and BIP-2, a significant database of iodine deposition data and organic iodide production data was accumulated. These data have contributed to the development of iodine models at organisations around the world. However, many key questions surrounding iodine behaviour in containment remain unresolved, and additional data are required to both improve knowledge of iodine-paint interactions and to assist in further model development and validation activities [4].

BIP-3 focused on outstanding questions remaining from BIP-1 and 2 and addressed knowledge gaps that arise when attempting to extrapolate results to postulated nuclear accident conditions. Additionally, one of the conclusions made by delegates at the 2015 NEA International Iodine Workshop (held in Marseille, France) was that the execution of collaborative analytical activities has been limited in recent years. In response, the BIP- 3 programme was structured to include both experimental and analytical activities within the scope of work.

The main objectives for BIP-3 were to:

- perform experiments that will resolve outstanding questions and improve the simulations of BIP and STEM results, including:
  - improve our ability to simulate iodine adsorption and desorption on containment surfaces;
  - predict CH_3I behaviour under accident conditions;
  - investigate the effect of paint ageing on these processes.
- further investigate the effect of contaminants (NO_2, Cl_2);
- share simulation strategies through modelling exercises (with member participation).

2.2. BIP-3 experimental tests performed

Three main iodine phenomena were studied experimentally in BIP-3 in support of the project objectives described previously, and are summarised below:

1. Iodine sorption onto painted surfaces. Tests have evaluated the effects of the following parameters:
   - paint ageing strategy (natural, pre-irradiation, thermal);
   - substrate type (Amerlock, Ripolin, Epigrip and Gehopon paints; scoping tests with glass, O-ring materials);
   - presence of contaminant species (e.g. NO_2, Cl_2);
   - other parameters such as loading [I_2], surface loading concentration, humidity, temperature.
2. Radiolytic organic iodide production from iodine-loaded coupons. Tests have evaluated the effects of the following parameters:
   - paint ageing strategy (e.g. natural, pre-irradiation, thermal);
   - presence of contaminant species (e.g. NO_2, Cl_2) during loading;
   - presence of water;
   - revolatilisation from glass, or production from other available organic sources (O-ring).
3. The potential for gas phase CH_3I production from I_2 and CH_4.

A particular focus of BIP-3 was to evaluate the influence of paint ageing and pre-treatment strategies on sorption behaviour and organic iodide production [5]. To date, many iodine experiments have used paint that could be considered quite fresh in comparison with in-service containment coatings. Questions remain regarding the applicability of such results to in-service containment coatings, which may be exposed to constant low-level operational radiation fields, or may be decades old. Experiments in BIP-3 evaluated how different ageing strategies such as heat treatments, pre-irradiation and natural ageing impact the amount of releasable carbon from the paint, the rate of iodine adsorption onto the painted surface, and the production of methyl iodide (as a surrogate for all volatile organic iodides) during irradiation of the test samples. While most tests were performed with Amerlock painted coupons, a limited number of tests with Gehopon, Ripolin, and Epigrip paints were also performed at the request of the programme review group (PRG) members.

Several experiments also expanded on previous themes and topics of interest in BIP-1 and BIP-2. A final test was performed to evaluate the role of water in the organic iodide production mechanism, simulating the scenario of condensation or sprays in containment that will lead to wetting of the painted walls after gaseous iodine loading. The impact of pre-exposing painted coupons to reactive gases was also studied using higher concentrations and longer exposure periods than those used for BIP-2 to determine if sufficiently high NO_2 or Cl_2 concentrations will eventually start to compete with iodine for active sites on the paint.

Tests to assist in the interpretation and modelling of BIP and STEM data were also performed. The interactions of iodine with glass and O-ring surfaces were explored. Iodine sorption studies, methyl iodide production from the O-ring, and the revolatilisation of adsorbed iodine from glass surfaces to generate methyl iodide (either through direct release of adsorbed CH_3I, or release as I_2 with subsequent reaction with gaseous organic contaminants in air) were completed.

Experiments in BIP-3 also studied the sorption behaviour of iodine as a function of the total iodine loading. These experiments were needed to determine whether the amount of physisorbed iodine increases as the chemisorption sites become occupied. Given that paint is a major iodine sink within containment, this information was considered important for model development.

Similarly, the importance of gas phase CH_3I production from the irradiation of methane-iodine gas mixtures has been debated in the open literature. Although it is generally believed that O_2 will outcompete I_2 for any $^{\bullet}CH_3$ radicals, some references have suggested methyl iodide production can be significant in such mixtures [6][7]. Tests were performed in BIP-3 to confirm whether this process can significantly impact the gas phase speciation of iodine in post-accident containment.

Overall, nearly 100 tests were performed in the BIP-3 programme, with approximately 25% of the tests having been added to the test matrix over the project life. Detailed descriptions of the tests performed are provided in Section 2.3.

2.3. BIP-3 experimental test matrix

Five experimental series, in addition to a small number of scoping tests, were performed in the BIP programme to address the phenomena identified in Section 2.2 and they are briefly described in Table 2.1. A summary of specific tests performed in support of each series, along with relevant experimental details, are provided in Table 2.2 through Table 2.6.

For TOC, AD and RAD tests (Table 2.1) with Amerlock coupons, test names generally include the test series (e.g. AD), the coupon pre-treatment description (e.g. NO_2 to indicate a coupon pre-exposed to NO_2), and a serial number to identify replicate tests. As an example, AD-PRE1-2 represents the second replicate adsorption test for an Amerlock coupon that has been pre-irradiated to 100 kGy total absorbed dose. For AD and RAD tests with other paint types, a similar convention is used, except that an additional paint identifier is included after the test series identifier. For example, RAD-RIP-PRE1-1 is the first replicate irradiation test performed on Ripolin coupons that have been pre-irradiated to 100 kGy total absorbed dose. The DES series tests identify different target loadings using sequential numbering after the paint identifier. For example, DES-AMER-2-1 is the first replicate of the DES series adsorption test performed on an Amerlock coupon using target loading condition #2 (2E-04 mol/dm^2). Because the METH series tests (Table 2.1) do not involve painted coupons, a simple sequential numbering scheme was used, with A, B, C, etc. used to identify replicate tests.

Table 2.1. Test series completed within the BIP-3 project

Test Series	Description
TOC	Solvent leaching tests performed on fresh and aged Amerlock coupons to evaluate the total organic carbon (TOC) and total inorganic carbon (TIC) release to water following 302 hours of exposure.
DES	Adsorption tests performed on fresh Amerlock coupons to varied target I_2 loading concentrations on the coupon surface.
AD	Adsorption tests performed on painted coupons, glass coupons or O-ring material under various conditions.
RAD	Irradiation tests performed on painted coupons or O-ring material to evaluate methyl iodide (CH_3I) production with time.
METH	Irradiation tests (and select blank, non-irradiated tests) to evaluate the potential gaseous reaction between I_2 and CH_4 (a surrogate volatile organic compound).
Other	Scoping tests to evaluate other specific interactions, such as CH_3I adsorption onto glass and O-ring surfaces; impact of the vessel rinsing procedure on iodine transfer to vessel O-ring.

Source: CNL, 2020.

Table 2.2. Summary of all TOC series tests performed in the BIP-3 project

Test name		Coupon material	Description
Blank (Room Temp.)		No coupons	Water at room temperature.
Blank (65 °C)		No coupons	Water at 65 °C
TOC-FRESH-1		Amerlock	2 coupons, painted 2015, 60 mL water at 65 °C
TOC-2013-1		Amerlock	2 coupons , painted 2013, 60 mL water at 65 °C
TOC-2009-1		Amerlock	2 coupons, painted 2009, 60 mL water at 65 °C
TOC-TC1-1		Amerlock	2 coupons, heat treatment 1 (130°C for 96 h), 60 mL water at 65 °C
TOC-TC2-1		Amerlock	2 coupons, heat treatment 2 (130°C + water for 96 h), 60 mL water at 65 °C
TOC-PRE1-1		Amerlock	2 coupons, pre-irradiation to 100 kGy, 60 mL water at 65 °C
TOC-PRE2-1		Amerlock	2 coupons, pre-irradiation to 1 000 kGy, 60 mL water at 65 °C

Source: CNL, 2020.

Table 2.3. Summary of all DES series tests performed in the BIP-3 project

Test name	Coupon material	Pre-treatment	Loading temp. (°C)	Loading RH (%)	Loading [I_2] (M)	Target Iodine Loading (mol/dm^2)	Other information
DES-AMER-1-1 DES-AMER-1-2	Amerlock	None	70	70	1.00E-07 5.00E-08	2E-03	Painted 2015
DES-AMER-2-1 DES-AMER-2-2	Amerlock	None	70	70	2.00E-08 1.00E-08	2E-04	Painted 2015
DES-AMER-3-1	Amerlock	None	70	70	2.00E-08	2E-05	Painted 2015
DES-AMER-4-1 DES-AMER-4-2	Amerlock	None	70	70	1.00E-09 1.00E-09	2E-06	Painted 2015
DES-AMER-5-1 DES-AMER-5-2	Amerlock	None	70	70	1.00E-09 1.00E-09	2E-07	Painted 2015

Source: CNL, 2020.

Table 2.4. Summary of all AD series tests performed in the BIP-3 project. Unless otherwise noted, each adsorption test was performed with three coupons

Test name	Coupon material	Loading temp. (°C)	Loading RH (%)	Loading $[I_2]$ (M)	Other information
Tests related to ageing phenomena:					
AD-FRESH-1	Amerlock	70	70	1E-08	Painted 2015
AD-FRESH-2	Amerlock	70	70	1E-08	Painted 2015
AD-FRESH2-1	Amerlock	70	70	1E-08	Painted 2018
AD-FRESH2-2	Amerlock	70	70	1E-08	Painted 2018
AD-FRESH2-3	Amerlock	70	70	5E-08	Painted 2018, Higher iodine loading concentration
AD-FRESH2-80-1	Amerlock	80	15 40 60	1E-08	Painted 2018, No desorption phase between loadings
AD-2013-1	Amerlock	70	70	1E-08	Painted 2013
AD-2009-1	Amerlock	70	70	1E-08	Painted 2009
AD-PRE1-1	Amerlock	70	70	1E-08	100 kGy pre-irradiation
AD-PRE2-1	Amerlock	70	70	1E-08	1 000 kGy pre-irradiation
AD-TC1-1	Amerlock	70	70	1E-08	Heat treatment 1 (130°C for 96 h)
AD-TC1-2	Amerlock	70	70	1E-08	Heat treatment 1 (130°C for 96 h)
AD-TC2-1	Amerlock	70	70	1E-08	Heat treatment 2 (130°C + water, 96 h)
AD-PRE2TC2-1	Amerlock	70	70	1E-08	1 000 kGy pre-irradiation followed by heat treatment 2 (130°C + water, 96 h)
AD-PRE2TC2-2	Amerlock	70	70	1E-08	1 000 kGy pre-irradiation followed by heat treatment 2 (130°C + water, 96 h)
AD-PRE2TC3-1	Amerlock	70	70	1E-08	1 000 kGy pre-irradiation followed by heat treatment 3 (160°C + water, 96 h)
Tests with other containment paints:					
AD-RIP-PRE1-1	Ripolin	70	70	1E-08	100 kGy pre-irradiation
AD-RIP-PRE2-1	Ripolin	70	70	1E-08	250 kGy pre-irradiation
AD-RIP-PRE3-1	Ripolin	70	70	1E-08	500 kGy pre-irradiation
AD-RIP-PRE4-1	Ripolin	70	70	1E-08	1 000 kGy pre-irradiation
AD-EPI-2010-1	Epigrip	70	70	1E-08	Painted 2010, Natural ageing
AD-GEH-A0-1	Gehopon	80	15 40 60	1E-08	Received 2013, natural ageing, no desorption phase between loadings
AD-GEH-A0-2[(a)]	Gehopon	80	15 40 60	1E-08	Replicate with desorption phase, run performed with only two coupons

Source: CNL, 2020.

Table 2.4. Summary of all AD series tests performed in the BIP-3 project. Unless otherwise noted, each adsorption test was performed with three coupons (Continued)

Test name	Coupon material	Loading temp. (°C)	Loading RH (%)	Loading [I_2] (M)	Other information
AD-GEH-A30-1	Gehopon	80	15 40 60	1E-08	Received 2013, simulated ageing (155°C for 42 h), no desorption phase between loadings.
AD-GEH-A30-2[(a)]	Gehopon	80	15 40 60	1E-08	Replicate with desorption phase, run performed with only one coupon.
Tests with pre-exposures to reactive gases:					
AD-NO2-1-1	Amerlock	70	70	1E-08	Painted 2018, Pre-exposure to 245 ppm NO_2 at 70°C/70% RH for 4h.
AD-NO2-2-1	Amerlock	70	70	5E-08	Painted 2018, Pre-exposure to 245 ppm NO_2 at 70°C/70% RH for 4h.
AD-Cl2-1-1	Amerlock	70	70	1E-08	Painted 2018, Pre-exposure to 245 ppm Cl_2 at 70°C/70% RH for 4h.
Tests with materials other than paint:					
AD-RIG-1	N/A[(b)]	70	70	1E-08	No coupons, empty sample chambers.
AD-RIG-2	Glass[(c)]	30	15 40 60	1E-08	Two glass coupons, one empty sample chamber.
AD-RIG-3(a,b,c)	Glass[(c)]	30	60	1E-08	Two glass coupons, one empty sample chamber. (a) 1 h (b) 2 h and (c) 6 h loading times
AD-RIG-4(a,b,c)	Glass[(c)]	70	70	1E-08	Two glass coupons, one empty sample chamber. (a) 1 h (b) 2 h and (c) 6 h loading times
AD-ORING-1	O-ring[(d)]	70	70	1E-08	Three silicone O-ring pieces.

Source: CNL, 2020.

(a) Because of limited remaining Gehopon A0 and A30 coupon inventory, runs AD-GEH-A0-2 and AD-GEH-A30-2 were completed simultaneously by placing two A0 coupons and one A30 coupon in the available sample chambers.

(b) No coupons were placed in the sample holders. Online measurements are representative of the iodine adsorbing onto the empty sample holders.

(c) Glass coupons were placed into two of the sample holders, while the remaining sample holder was left empty for comparison.

(d) Three 0.5 inch-long pieces of a silicone O-ring (the material used to seal the old BIP irradiation vessel) were placed into the sample holders.

Table 2.5. Summary of all RAD series tests performed in the BIP-3 project. Unless otherwise noted, tests were performed with six iodine-loaded coupons in the irradiation vessel

Test name	Coupon material	Loading temp. [(a)] (°C)	Loading RH [(b)] (%)	Dose rate[(c)] (kGy/h)	Other information
RAD-FRESH-1	Amerlock	70	70	0.75	Painted 2015
RAD-FRESH2-1-NV	Amerlock	70	70	0.59	Painted 2018
RAD-FRESH2-2-NV	Amerlock	70	70	0.53	Painted 2018 Phase 1: Irradiation of coupons after gas load
		N/A	N/A	0.53	Phase 2: Irradiation of empty vessel (coupons removed) to check for revolatilisation of deposits
RAD-2013-1	Amerlock	70	70	0.75	Painted 2013
RAD-2013-2	Amerlock	70	70	0.65	Painted 2013
RAD-2013-3-NV	Amerlock	70	70	0.57	Painted 2013
RAD-2009-1	Amerlock	70	70	0.74	Painted 2009
RAD-2009-2-NV	Amerlock	70	70	0.56	Painted 2009
RAD-PRE1-1	Amerlock	70	70	0.74	100 kGy pre-irradiation
RAD-PRE1-2	Amerlock	70	70	0.67	100 kGy pre-irradiation
RAD-PRE1-3-NV	Amerlock	70	70	0.60	100 kGy pre-irradiation
RAD-PRE1-4-NV	Amerlock	70	70	0.60	100 kGy pre-irradiation
RAD-PRE2-1	Amerlock	70	70	0.73	1 000 kGy pre-irradiation
RAD-PRE2-2	Amerlock	70	70	0.67	1 000 kGy pre-irradiation
RAD-PRE2-3-NV	Amerlock	70	70	0.57	1 000 kGy pre-irradiation
RAD-TC1-1	Amerlock	70	70	0.66	Dry heat treatment
RAD-TC2-1	Amerlock	70	70	0.72	Heat/steam treatment (130°C)
RAD-TC2-2-NV	Amerlock	70	70	0.55	Heat/steam treatment (130°C)
RAD-PRE2TC2-1	Amerlock	70	70	0.63	1 000 kGy pre-irradiation and heat/steam treatment (130°C) Phase 1: Irradiation of coupons after gas load
		N/A	N/A	0.63	Phase 2: Vessel O-ring from Phase 1 placed into a clean vessel (no coupons) and irradiated
RAD-PRE2TC3-1-NV	Amerlock	70	70	0.54	1 000 kGy pre-irradiation and heat/steam treatment (160°C) Phase 1: Irradiation of coupons after gas load
		N/A	N/A	0.54	Phase 2: Irradiation of empty vessel (coupons removed) to check for revolatilisation of deposits
RAD-ORING-1-NV	Silicone O-ring	70	70	0.58	Pieces of silicone O-ring, used to seal older irradiation vessel design. Surface area of each piece was estimated to be 1.85 cm^2.
RAD-RIP-FRESH-1	Ripolin	70	70	0.59	No pre-irradiation applied Coupons received July 2017
RAD-RIP-PRE1-1	Ripolin	70	70	0.65	100 kGy pre-irradiation
RAD-RIP-PRE4-1	Ripolin	70	70	0.64	1 000 kGy pre-irradiation Phase 1: Irradiation of coupons after gas load

Source: CNL, 2020.

Table 2.5. Summary of all RAD series tests performed in the BIP-3 project. Unless otherwise noted, tests were performed with six iodine-loaded coupons in the irradiation vessel (Continued)

Test name	Coupon material	Loading temp. [(a)] (°C)	Loading RH [(b)] (%)	Dose rate[(c)] (kGy/h)	Other information
RAD-PRE2TC3-1-NV	Amerlock	70	70	0.54	1 000 kGy pre-irradiation and heat/steam treatment (160°C) Phase 1: Irradiation of coupons after gas load
		N/A	N/A	0.54	Phase 2: Irradiation of empty vessel (coupons removed) to check for revolatilisation of deposits
RAD-ORING-1-NV	Silicone O-ring	70	70	0.58	Pieces of silicone O-ring, used to seal older irradiation vessel design. Surface area of each piece was estimated to be 1.85 cm^2.
RAD-RIP-FRESH-1	Ripolin	70	70	0.59	No pre-irradiation applied Coupons received July 2017
RAD-RIP-PRE1-1	Ripolin	70	70	0.65	100 kGy pre-irradiation
RAD-RIP-PRE4-1	Ripolin	70	70	0.64	1 000 kGy pre-irradiation Phase 1: Irradiation of coupons after gas load
		N/A	N/A	0.64	Phase 2: Vessel O-ring from Phase 1 placed into a clean vessel (no coupons) and irradiated
RAD-AMER-WET-1	Amerlock	70	70	0.65	16 h water soak after gas load
RAD-AMER-WET-2	Amerlock	70	70	0.64	Phase 1: Irradiation after gas load
		N/A	N/A	0.64	Phase 2: After Phase 1 irradiation, coupons are soaked in water for 16 h, then irradiated a second time in a clean vessel (new O-ring).
RAD-NO2-1-1-NV	Amerlock	70	70	0.52	Coupon pre-exposure to 245 ppm NO_2 at 70°C, 70% RH for 4 h, followed by I_2 loading at 70°C, 70% RH, 1×10^{-8} M I_2. Phase 1: Irradiation of coupons after gas load.
		N/A	N/A	0.52	Phase 2: Irradiation of empty vessel (coupons removed) to check for revolatilisation of deposits.
RAD-NO2-2-1-NV	Amerlock	70	70	0.53	Coupon pre-exposure to 245 ppm NO_2 at 70°C, 70% RH for 4 h, followed by I_2 loading at 70°C, 70% RH, 5×10^{-8} M I_2. Phase 1: Irradiation of coupons after gas load.
		N/A	N/A	0.64	Phase 2: Vessel O-ring from Phase 1 placed into a clean vessel (no coupons) and irradiated.
RAD-AMER-WET-1	Amerlock	70	70	0.65	16 h water soak after gas load.
RAD-AMER-WET-2	Amerlock	70	70	0.64	Phase 1: Irradiation after gas load.
		N/A	N/A	0.64	Phase 2: After Phase 1 irradiation, coupons are soaked in water for 16 h, then irradiated a second time in a clean vessel (new O-ring).
RAD-NO2-1-1-NV	Amerlock	70	70	0.52	Coupon pre-exposure to 245 ppm NO_2 at 70°C, 70% RH for 4 h, followed by I_2 loading at 70°C, 70% RH, 1×10^{-8} M I_2. Phase 1: Irradiation of coupons after gas load.
		N/A	N/A	0.52	Phase 2: Irradiation of empty vessel (coupons removed) to check for revolatilisation of deposits.
RAD-NO2-2-1-NV	Amerlock	70	70	0.53	Coupon pre-exposure to 245 ppm NO_2 at 70°C, 70% RH for 4 h, followed by I_2 loading at 70°C, 70% RH, 5×10^{-8} M I_2. Phase 1: Irradiation of coupons after gas load.

Source: CNL, 2020.

(a) Temperature during the loading phase; samples were irradiated at ambient temperature.

(b) Relative humidity during the loading phase; samples were irradiated with no control of humidity.

(c) As measured by Fricke dosimetry.

Table 2.6. Summary of all METH series tests performed in the BIP-3 project

Test name	CH_4 (ppm)	I_2 (M)	Cover gas	Water (ml)	Dose rate[(a)] (kGy/h)	Other information
METH-1	~7%	High	Air	0	0.82	I_2(s) present in vessel.
METH-2	200	1e-6	Air	0	0.79	
METH-2B	200	1e-6	Air	0	0.78	
METH-2 Blank	200	1e-6	Air	0	0	Non-irradiated blank.
METH-3	200	1e-6	N_2	0	0.79	
METH-3B	200	1e-6	N_2	0	0.78	
METH-4	200	1e-6	Air	5	0.79	
METH-4B	200	1e-6	Air	5	0.78	
METH-10	200	1e-7	Air	0	0.77	
METH-10B	200	1e-7	Air	0	0.77	
METH-10 Blank	200	1e-7	Air	0	0	Non-irradiated blank. Kept in dark.
METH-0	0	1e-7	Air	0	0.77	
METH-11	200	1e-8	Air	0	0.77	
METH-11B	200	1e-8	Air	0	0.77	
METH-11 Blank	200	1e-8	Air	0	0	Non-irradiated blank. Kept in dark.

Source: CNL, 2020.

(a) Dose rate as measured by the Fricke dosimeter. An adjustment may be necessary to account for different mass-energy adsorption coefficients between Fricke solution and air.

2.4. Overview of BIP-3 Analytical Working Group (AWG) modelling exercises

The BIP-3 AWG was assembled with the general mandate to encourage discussion of modelling strategies and to provide guidance to ongoing experimental and code development work regarding the two main aspects of the iodine-paint interaction studied across all of the BIP programmes:

1. iodine adsorption/desorption from surfaces, and
2. organic iodide production from irradiated epoxy surfaces.

The BIP-3 AWG scope of work was performed in conjunction with the OECD BIP-3 research programme from January 2016 through June 2018 and involved the completion of two independent modelling exercises where the BIP-3 members were encouraged to participate and share modelling data for selected scenarios. The modelling exercises were performed in two stages, with Stage 1 being defined and led by the CNL (the operating agent) and Stage 2 being led by staff from the Institut de Radioprotection et de Sûreté Nucléaire (IRSN) who also chaired the BIP-3 AWG meetings.

Stage 1: Perform a co-operative sensitivity study based on a simple geometry and accident scenario (the same geometry was also used for a STEM-2 AWG activity).

Stage 2: Perform modelling of two selected benchmark tests: RAD-EPICUR-A1 from the BIP-2 Programme, and LD3 from the STEM Programme.

Representative organisations from seven of the BIP-3 member countries participated in the AWG modelling exercises. Six different computational codes were used to model the selected

scenarios, including commercially-available severe accident codes, such as ASTEC, MELCOR, and COCOSYS, and research codes or codes developed and maintained internally by the participating organisation, including LIRIC, INSPAIR and KICHE(OrgIDB). Detailed descriptions of the respective codes and participant submissions are available in the AWG Summary report [8]. A brief overview of the Stage 1 and Stage 2 modelling exercises is provided in the sections below.

2.4.1. Overview of the Stage 1 modelling exercise

The main objective of the Stage 1 modelling exercise was to demonstrate the sensitivity of the simulated total airborne iodine to the inclusion of sub-models related to the radiolytic formation of organic iodides from iodine-loaded paint.

A simple scenario was devised to include conditions somewhat representative of a severe accident, while excluding issues that could complicate the iodine calculation and detract from the main objective. The simulation scenario assumed a loss of primary coolant followed by fuel failure and release of fission products. Iodine chemistry occurring in the containment building was calculated starting from a time when iodine-containing aerosols and other fission products have settled and have been washed into a water pool. It was assumed that the majority of the iodine entered containment as non-volatile I^-, although a small portion (~2.5%) was assumed to enter the containment building as I_2. The conditions chosen for the Stage 1 simulation are summarised in Table 2.7.

Participants were asked to perform simulations using the conditions outlined in Table 2.7 with and without the formation of organic iodide from irradiated painted surfaces being considered in the simulation. The following outputs were requested for each modelling submission in Stage 1:

- total gas phase iodine;
- gas phase iodine speciation (I_2, ORGI, IOx, etc.);
- total aqueous iodine;
- aqueous iodine speciation (major species if available);
- pool pH evolution (if pH is changing);
- surface loading (submerged surface, dry surface, etc.).

The objectives of this modelling exercise were to:

- evaluate the significance of the iodine-paint interaction in available models to predict iodine volatility;
- evaluate the relevance of gaseous radiolytic reactions involving organic compounds (like CH_4) and gaseous I_2 and the need to include these phenomena for future model development;
- identify the remaining uncertainties in iodine-paint interaction models and gas phase iodine chemistry.

Table 2.7. Simulation base conditions for the Stage 1 co-operative sensitivity study

Parameter	Value	Rationale/Comments
Vessel geometry	Cylinder	A common containment shape
Total volume	52 000 m^3	Similar to CANDU 6 and French reactor designs
Water volume	2 000 m^3	Total of heat transport and emergency water
Gas volume	50 000 m^3	Similar to CANDU 6 and French reactors
Water-gas interface area	1 350 m^2	Cross-sectional area of a cylinder with a diameter of 41.46 m (CANDU 6)
Painted surface area (dry)	25 000 m^2	Assume all surfaces are painted
Painted surface area (wet)	1 350 m^2	Floor area
Inert surface area	0 m^2	Can consider as sensitivity case
Steel surface area	0 m^2	Can consider as sensitivity case
Temperature	100 °C	Within the range of a severe accident
Relative humidity (RH)	70 %	RH might be higher in reality, but data is available at 70%
Dose rate to gas phase	1 kGy/h	Within the estimated range of post-accident dose rates
Dose rate to water	1 kGy/h	Within the estimated range of post-accident dose rates
Thermalhydraulics	Vigorous mixing in both phases	To maintain homogeneity
pH evolution	Controlled at 9.0 for 84 h, then step change and controlled at 5.0 for 84 h	Most reactor sumps will be initially alkaline, but will acidify with time (e.g. organic radiolysis and nitric acid formation)
Initial water chemistry	Pure water	Avoid complications with trisodium phosphate (TSP), boric acid, etc.
Initial iodine species	Aqueous: 1e-5 M I^- (aq) Gas: 5e-9 M I_2 (g)	~97.5% of the iodine enters containment as a soluble form (e.g. CsI) and ~2.5% enters containment in the form of I_2. Total mass is 2 603.5 g iodine
Atmosphere	Normal air (with no CO_2)	CO_2 not present to affect pH for simulation
Other chemical changes	None, other than what is needed to affect the pH change	For simplicity

Source: CNL, 2020.

2.4.2. Overview of the Stage 2 modelling exercises

Stage 2 of the BIP-3 AWG included the modelling of two benchmark tests related to iodine-paint interactions:

1. STEM test LD3 (on-line test). This test was performed in the IRSN facility and the data was released to BIP-3 AWG participants for use in this study [9].
2. BIP-2 test RAD-EPICUR-A1 (batch test). This test was performed in the CNL iodine research facility [10].

Specific details regarding the benchmark tests are described in the respective STEM and BIP-2 project reports [9][10]. A summary of the experimental conditions for the two benchmark tests is provided in Table 2.8.

Table 2.8. Summary of experimental conditions for STEM Test LD3 and BIP-2 Test RAD-EPICUR-A1

Parameter	STEM, Test LD3	BIP-2, Test RAD-EPICUR-A1
Epoxy painted coupon surface (cm²)	50	30.4
Temperature (°C)	80 ± 2	80
Pressure (bars)	1.70 ± 0.05	1.0
Relative humidity (%)	60 ± 3	Ambient (not controlled)
Vessel volume (L)	4.8	0.93
Vessel surface (cm²)	1 550 (steel)	870 (glass)
Dose rate (Gy/s)	Gas phase: 0.46 ± 0.04 Coupon level: 0.33 ± 0.03	0.325
Initial $[I]_{ads}$ on the paint (mol/m²)	$(9.50 \pm 0.20)\times10^{-5}$	1.46×10^{-3}
Gaseous flow rate in the vessel (L/min)	0.250 ± 0.005	0
Pre-irradiation sweeping phases (h)	0	0
Irradiation phase duration (h)	30 h	138 h (loaded coupons) 142 h (non-loaded coupons)
Post-irradiation sweeping phases (h)	5 h – air with 50% RH 1 h – dry air	0

Source: CNL, 2020.

3. Experimental methodology

3.1. Coupon preparation

3.1.1. Coupon fabrication, geometry and painting

To maintain consistency with earlier work and allow direct comparisons to BIP-1 and BIP-2 results, the CNL standard coupon geometry of ½ inch (1.27 cm) diameter and ¼ inch (0.635 cm) thickness was used whenever possible. The surface area of the CNL standard coupon geometry is approximately 5.08 cm^2. Coupons used in BIP-3 were fabricated from 304 L stainless steel, and were subsequently painted using the methodology below. A small number of adsorption tests were also performed using glass coupons (Schott Duran borosilicate glass) of the same dimensions.

Painted coupons were prepared prior to the start of the BIP-3 project (2015) by spray-coating with the appropriate coating(s) according to the paint manufacturer's specifications and allowing for the recommended curing times between successive layers. Amerlock 400 coupons were prepared by coating the stainless steel coupons with three layers of the paint (no undercoat) to a total average thickness of 0.18 mm. This treatment was similar to that used for earlier coupon batches painted for BIP-1 and BIP-2. The coupons painted in 2015 were considered fresh (denoted "FRESH") for subsequent experimental work.

At the conclusion of Year 2, the inventory of FRESH Amerlock coupons (painted in 2015) was limited and a new batch of coupons was prepared to replenish the supply in accordance with the method outlined above. To distinguish between the different batches of coupons, tests using the new batch of coupons (painted 2018) were denoted "FRESH2", or their use is otherwise noted in the test matrix information (Section 3.3).

3.1.2. Paint ageing techniques and pre-treatments for Amerlock coupons

The effect of different paint ageing techniques on the sorption behaviour and organic iodide production arising from painted coupons was evaluated in BIP-3. The ageing strategies are summarised in Sections 3.1.2.1 to 3.1.2.4 below.

3.1.2.1 Natural ageing of painted coupons

A limited stock of naturally-aged Amerlock coupons was available for testing. These coupons were originally prepared for BIP-1 (painted 2009) and BIP-2 (painted 2013), and have been stored in the laboratory. Freshly prepared Amerlock coupons (painted 2015, 2018) were also used for comparison.

3.1.2.2 Pre-irradiation of painted coupons

Painted coupons (painted in 2015) were placed in a beaker (Figure 3.1) and irradiated within a Gammacell-220 ^{60}Co irradiator[2] at a dose rate of 0.86 kGy/h up to total absorbed doses of 100 kGy (Pre-irradiation 1 [PRE1]) and 1 000 kGy (Pre-irradiation 2 [PRE2]).

2. The Gammacell-220 ^{60}Co irradiator was distributed by MDS Nordion.

Figure 3.1. Set-up used for coupon pre-irradiations

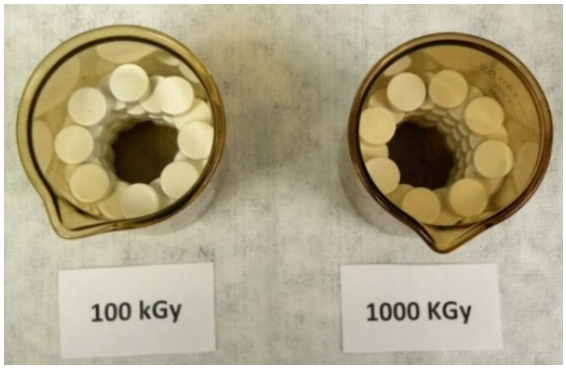

Source: CNL, 2020.

3.1.2.3 Thermal curing pre-treatments

Thermal pre-treatments are often used to simulate the effects of paint ageing [11][12]. Two thermal curing strategies were selected for use in BIP-3: (1) thermal curing performed under dry conditions, and (2) thermal curing performed in a water-saturated environment.

For Thermal Cure 1 (TC1), the coupons were placed into open glass vials and were heated to 130±2 °C for 96 hours in an oven (ambient air conditions).

For Thermal Cure 2 (TC2), coupons were suspended in glass holders within a 2 L Autoclave Engineers Hastalloy C autoclave outfitted with a 3 kW heater. Excess water was added (100 mL) to ensure saturated steam conditions upon heating and coupons were suspended well above the water level. The temperature was increased to 130°C within about 2 h and was controlled at 130°C to within about 4°C. After 96 h the heating was discontinued and the vessel was allowed to cool. Coupons were stored in capped glass vials until required for testing (within 2 days). The autoclave water was sampled at the end of the second run containing six coupons for RAD-TC2-1. The total organic carbon was measured to be 118.4 mg C/L.

Coupons were observed to change colour as a result of the thermal curing process (Figure 3.2).

Figure 3.2. Coupons before and after the thermal cure processes

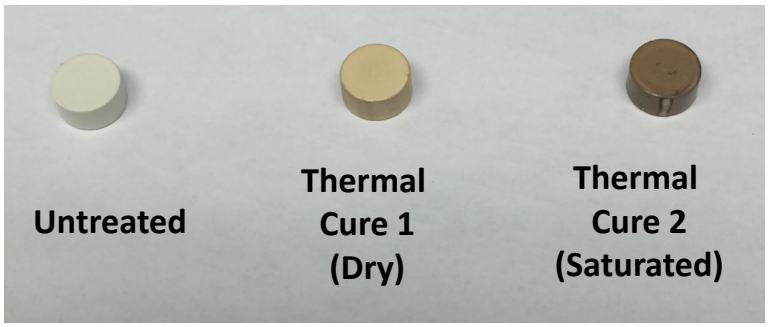

Source: CNL, 2020.

Thermal Cure 2 affected the coating integrity in such a way that a small amount of the underlying steel was visible after coupons were removed from the glass holders (coupons had some adherence to the glass, and the coating chipped during manipulation).

3.1.2.4 Combined ageing strategies – Pre-irradiation and thermal curing

To determine if the combination of ageing methods would have an additive effect on iodine sorption processes or organic iodide production, a small number of coupons were prepared using both a pre-irradiation and a sequential thermal curing treatment.

Coupons that had been pre-irradiated to 1 000 kGy (PRE2) were subsequently heated for 96 h in an autoclave at 130 °C under water-saturated conditions. This pre-treatment was defined as PRE2TC2.

Additionally, coupons that had been pre-irradiated to 1 000 kGy (PRE2) were subsequently heated for 96 h in an autoclave at 160 °C under water-saturated conditions (TC3). This pre-treatment was defined as PRE2TC3.

3.1.3. Ageing tests with other painted coupons

The original BIP-3 proposal did not include tests with other containment paints. However, a limited number of tests were added in consultation with the PRG to determine if other containment paints demonstrate similar ageing effects as observed for Amerlock paint.

3.1.3.1 Epigrip – Natural ageing

An inventory of Epigrip-painted coupons, which had originally been prepared in 2010 for testing in BIP-1, was still available. These coupons had been stored in the laboratory. Experimental results using the naturally-aged Epigrip coupons were compared to previous results from BIP-1.

3.1.3.2 Ripolin – Pre-irradiation

Ripolin-painted coupons were prepared by IRSN in France in accordance with the standard coupon geometry for BIP-3 (see Section 3.1.1). The coupons were received by the CNL in July 2017. Using the same process as described in Section 3.1.2.2, the Ripolin coupons were irradiated at 0.65 kGy/h to total absorbed doses of 100, 250, 500 and 1 000 kGy. The irradiated Ripolin coupons were noted to be slightly darker in colour than coupons that were not irradiated (Figure 3.3).

Figure 3.3. Ripolin coupons before and after irradiation

Source: CNL, 2020.

3.1.3.3 Gehopon – Natural ageing and combined natural and simulated ageing

A limited number of Gehopon-painted coupons (A0 and A30) were available which had originally been used for testing in BIP-2. Although prepared from the same batch, the A0 coupons remained untreated (natural ageing) while the A30 coupons had an artificial ageing treatment applied prior to their shipment to the CNL (155 °C for 42 h)[3] that was intended to simulate the effects of 30 years of ageing. Hence, the A30 coupons had experienced both simulated and natural ageing processes.

3.2. Iodine adsorption studies

Iodine can be adsorbed onto the coupon surfaces in one of two ways: (1) aqueous phase adsorption by immersing the samples in aqueous solutions containing iodine (as I_2), and (2) adsorption of gas phase elemental iodine from a stream of flowing air containing iodine vapour. For all experiments performed in BIP-3, only the gas phase adsorption technique was used.

Gas phase iodine adsorption and desorption onto surfaces were studied over a range of iodine concentrations, relative humidities (RH) and temperatures. The sorption experiments were carried out in the Radioiodine Adsorption Apparatus (Figure 3.4). In a typical test, three samples (in the form of coupons) were placed in glass flow cells (Figure 3.5) and exposed to a continuous flow of air containing ^{131}I-labelled I_2, followed by purging with iodine-free air. The adsorption cells are made of borosilicate glass to minimise iodine adsorption on the walls. The adsorption cells are situated in a heated oven chamber for temperature control. The iodine activity accumulated on each sample was continuously monitored during loading and purging using a γ-counting detector situated outside the oven and directly beneath each adsorption cell, see Figure 3.6. Small known fractions of the flows entering and leaving the adsorption cell were diverted to charcoal traps (referred to as the inlet and outlet trap, respectively). The ^{131}I activities accumulated in these traps were continuously monitored to determine the iodine loading and release concentrations in the inlet gas and in the effluent. The adsorption cells are disassembled at the end of each test and thoroughly cleaned before reuse. Further details of the experimental set-up and procedures are provided in Reference [13].

The uncertainty for typical activity-based measurements has been estimated as less than 15%, based on variations in the specific activity determined from a given batch of trace-labelled I_2. However, the uncertainty rises as the count rate becomes small.

Deposition velocities were extracted from the initial time periods of the collected adsorption curves. The length of time used for the deposition velocity calculation varied, depending on the curvature of the adsorption profiles and the data scatter, but was generally calculated from the first 3-6 hours of loading. After conversion to common units, the deposition velocity is calculated by simply dividing the loading rate by the loading concentration (Equation 1). For tests where desorption behaviour was monitored, the amount of desorbed iodine was also estimated from the measured changes in online surface activity.

$$\frac{Surface\ I_2 Loading\ rate\left(\frac{mol}{dm^2 \cdot s}\right)}{Gas\ Phase\ Concentration\left(\frac{mol}{dm^3}\right)} = Deposition\ velocity\ \left(\frac{dm}{s}\right) \quad (1)$$

3. Information regarding pre-treatment conditions were provided by GRS.

Figure 3.4. Schematic diagram of the multiple coupon Radioiodine Adsorption Apparatus. RH, T and P denote relative humidity, temperature and pressure transducers. UHP N_2 corresponds to ultra-high purity nitrogen

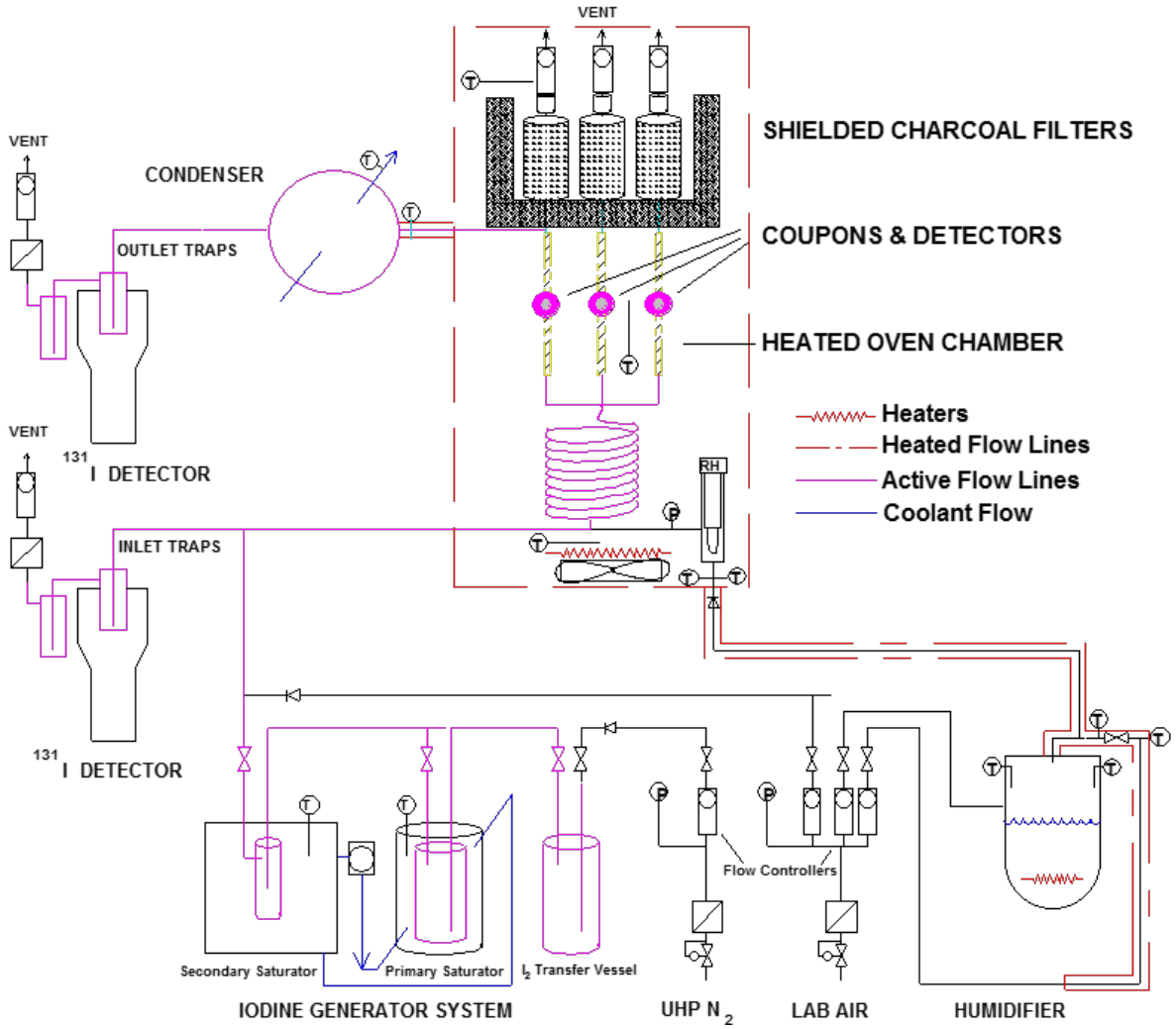

Source: CNL, 2020.

Figure 3.5. Top and side view of the adsorption cells

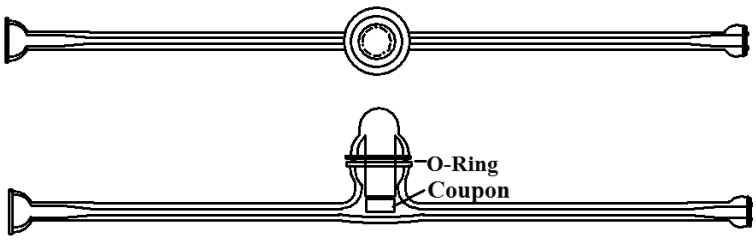

Source: CNL, 2020.

Figure 3.6. Cross-sectional diagram of the sample chambers and detectors

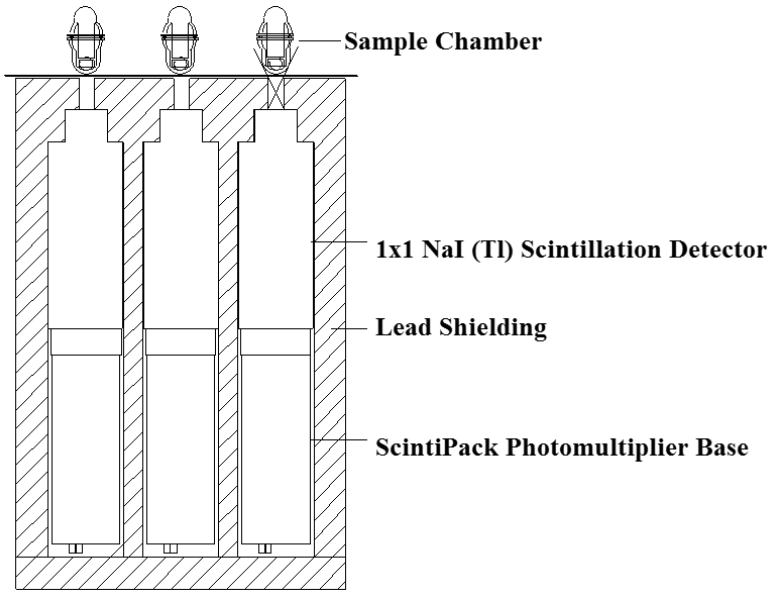

Source: CNL, 2020.

3.3. Irradiation tests to evaluate methyl iodide production

3.3.1. Irradiation vessels for RAD series tests

In these experiments, a glass vessel containing coupons that were pre-loaded with ^{131}I-labelled I_2 (as described in Section 3.2) and laboratory air was irradiated in a Gammacell-220 ^{60}Co irradiator for the purpose of evaluating the radiolytic formation of organic iodides. Six coupons were used for each irradiation test. Because only three coupons can be loaded at a time in the Radioiodine Adsorption Apparatus, the iodine loading was performed in two phases. Once loading of the first three coupons was complete, the coupons were transferred into scintillation vials where they were stored for the duration of the iodine loading for the second set of coupons. After the second loading phase was complete, all coupons were γ-counted to quantify the initial iodine loading on each coupon. The iodine-loaded coupons were then transferred into the irradiation vessel.

In BIP-1 and BIP-2, coupon irradiation tests had been performed using a glass vessel with an O-ring seal. This vessel was also used within the BIP-3 programme, and is described in Section 3.3.1.1. However, during the BIP-3 programme it became important to design a new vessel to eliminate the need for an O-ring seal, so as to reduce any contribution the O-ring may have on organic iodide production. The new O-ring free irradiation vessel is described in 3.3.1.2. Tests performed in the new vessel have been denoted 'NV'.

3.3.1.1 O-ring vessel for coupon irradiation tests

This vessel consists of upper and lower sections made from borosilicate glass (Schott Duran). Coupons are placed on custom glass holders that are suspended within the irradiation vessel, which is shown in Figure 3.7 and Figure 3.8. The two sections connect on inner and outer ground glass flanges. An O-ring (silicone) is positioned between the two ground glass surfaces. An external compression clamp ensures positive contact between the upper and lower sections. The upper section contains a screw cap port with a septum for gas sampling. With the coupon holders

and 6 coupons in place, the vessel volume contains 927 mL of gas space. The glass surface area (for the glassware shown in Figure 3.7) is estimated to be 870 cm^2. This estimate excludes contributions from the coupon holders.

Figure 3.7. Irradiation vessel (shown pre-irradiation and without the coupon holders)

Source: CNL, 2020.

Figure 3.8. Irradiation vessel (shown post-irradiation and with coupons and holders)

Source: CNL, 2020.

3.3.1.2 New irradiation vessel (without O-ring) for coupon irradiation tests

The O-ring was completely eliminated by designing a vessel with a 1 inch stainless steel tube with a glass/metal joint as the coupon access port (Figure 3.9 and Figure 3.10). The coupons in the most recent tests were held in a narrow glass holder, but were separated to promote contact and free exchange with the gas space. This change in design added an additional stainless steel surface area to the vessel, which may have retained a certain amount of iodine. However, previous tests performed in BIP-1 suggest the impact of this material addition to be small [14]. Complete elimination of the sampling septum was not possible because sample withdrawal is a necessary experimental activity. A stainless steel ball valve was added to separate the septum from the main irradiated volume thus eliminating the possibility of the septum as a contributor to radiolytic CH_3I production. The stainless steel ball valve contains a small amount of a Teflon-like material as seating for the rotating 'ball', which is not visible when the valve is open or closed, but could have a very small area in contact with the vessel atmosphere.

In order to accommodate the new valve/septum system, the height of the vessel needed to be decreased to fit within the Gammacell sample chamber; however, the new vessel volume is comparable to the previous vessel (1 060 mL compared to 927 mL for the O-ring vessel).

Figure 3.9. Diagram of new O-ring free irradiation vessel

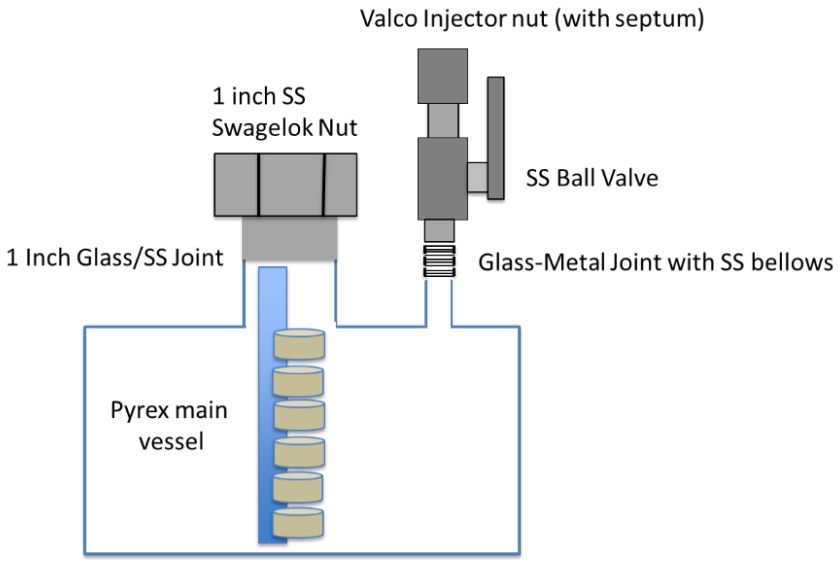

Source: CNL, 2020.

Figure 3.10. Photographs of the new O-ring free irradiation vessel and coupon holder design, with components disassembled (left) and fully assembled (right)

Source: CNL, 2020.

3.3.2. Irradiation vessel for METH series tests

A glass vessel (~1 L) optimised for gas experiments was used to study the gas phase production of methyl iodide from I_2 and CH_4 mixtures (Figure 3.11). The vessel had an inlet and an outlet

to facilitate gas purging, and ball valves (in addition to the septum) to ensure leak tightness. Due to the height of this vessel, and because the tests did not contain ^{131}I tracer, an alternate Gammacell located at the CNL site (with a similar dose rate) was used for these tests.

Figure 3.11. Irradiation vessel for gas phase experiments

Source: CNL, 2020.

3.3.3. Gas phase analysis

Sampling of the gas phase in the irradiation vessels was accomplished using a gas-tight syringe via the available gas sampling septum. Methyl iodide concentrations were determined by Gas Chromatography (GC). Gas samples were introduced into a 10 μL sample loop for injection into an HP 7890 Gas Chromatograph outfitted with a 30 m Agilent J&W DB-VRX capillary separation column (0.32 mm interior diameter) and an electron capture detector (ECD). The detection limit for CH_3I by this method was about 10^{-12} M. The practical detection limit, however, was higher (10^{-11} M) because of difficulties associated with reproducibility at low concentrations. Based on repeated injections of standard concentration, the uncertainty was estimated to be about 25% and increases for concentrations below 10^{-11} M.

For gas phase irradiation tests, the methane concentrations were also monitored with time. Methane concentrations were determined using the same GC system as described above, except a flame ionisation detector (FID), rather than an ECD, was used for the analysis. Because of this difference, methyl iodide and methane products could not be analysed simultaneously, and separate injections for each analysis were required.

3.3.4. Iodine desorption and mass balance analyses

After gas phase analyses were completed, the irradiation vessel was opened and the coupons were γ-counted to determine the amount of iodine desorbed by comparison to their pre-test loading. The vessel was then washed with three rinses of 20 mL 0.05 M NaOH. The wash solution was analysed for iodine content and was used for the mass balance calculation. The coupon holders for the various irradiation design are not rinsed and are not included in the mass balance calculation; however, they do represent a small percentage of the surface area. After the NaOH washes, the vessel was cleaned with methanol, acetone and propanol to dissolve any

remaining organic residue. Prior to the next experiment, the vessel was washed with pure water and baked at 500°C to remove residual organic contaminants.

3.3.5. Radiation dose rates

Dosimetry measurements were performed to estimate the dose rates to samples in BIP-3. The dose rate was measured to be 0.84 kGy/h as of January 2016 using the Fricke dosimeter (ferrous sulphate solutions). Dose rates for individual tests are provided in the data reports [13][15][16]. In BIP-1 and BIP-2, the dose rate was assigned a 17% uncertainty to account for variations in repeated tests and differences in geometry. A similar uncertainty was assigned for BIP-3.

4. Summary of BIP-3 experimental outcomes

This section provides an overview of the main experimental trends observed in BIP-3. Detailed experimental descriptions and discussions of specific test results can be found in the data reports [13][15][16].

4.1. Adsorption capacity

A series of iodine sorption tests were performed in BIP-3 to evaluate whether the fraction of physisorbed iodine is dependent on the total loading achieved. Sorption tests were performed for target loading concentrations spanning four orders of magnitude and, in order to achieve these loadings, the gaseous iodine concentration was also varied over two orders of magnitude. Upon examination of the data, it was determined that the iodine sorption behaviour was strongly associated with the gaseous iodine loading concentration used for the test. The dependence of the observed iodine desorption and the measured deposition velocity on the I_2 loading concentration are shown in Figure 4.1 and Figure 4.2, respectively.

In general, the relative amount of iodine desorption was observed to be greater for Amerlock coupons having higher initial surface loadings. Slower deposition velocities and larger fractions of desorbed iodine are measured when higher iodine gas concentrations were used during loading. Higher I_2 concentrations during loading appear to result in more loosely-bound or physisorbed I_2 on the paint surface.

Figure 4.1. Correlation between the gaseous iodine loading concentration and the relative amount of iodine desorbed for sorption tests on Amerlock

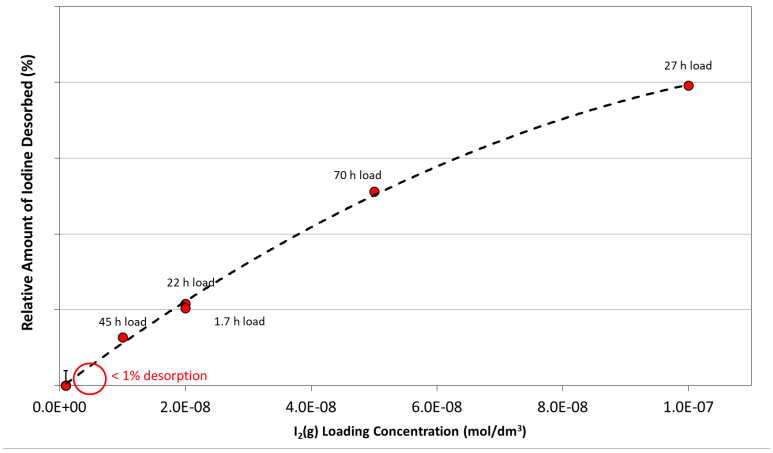

Source: CNL, 2020.

Figure 4.2. Correlation between the gaseous iodine loading concentration and the measured deposition velocity for sorption tests on Amerlock

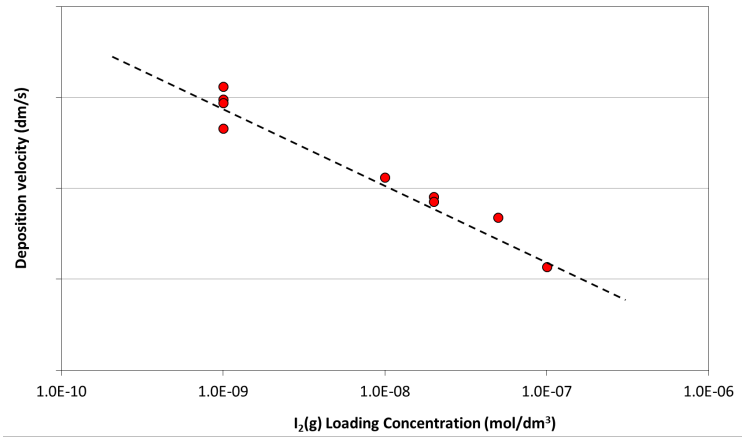

Source: CNL, 2020.

4.2. Paint ageing

Studies associated with evaluating the impact of different paint ageing strategies on iodine-paint interactions were a primary focus of BIP-3, and included sorption, irradiation and leaching experiments.

Natural ageing, pre-irradiation exposures to different adsorbed doses, and thermal curing treatments with and without steam were selected as the ageing strategies of interest for BIP-3. A limited number of tests were also performed on Amerlock painted coupons that had been both pre-irradiated and thermally-cured; for subsequent discussion, these tests will be termed combined ageing tests.

Figure 4.3 shows the iodine adsorption and desorption profiles measured on Amerlock for fresh, thermally-cured and combined ageing tests. As the deposition velocity is determined by the slope of the adsorption curve, it can be observed that the deposition velocity decreased slightly with time for all tests. Increased coupon ageing was shown to reduce the deposition velocity of iodine onto the paint, with thermal treatments involving water having a greater effect on the iodine deposition velocity than dry treatments. Combining ageing strategies appeared to have an additive effect, leading to greater reductions in deposition velocity than for any single ageing method. Measured deposition velocities for combined ageing tests were among the lowest measured across all BIP programmes.

Increased natural ageing and pre-irradiations to higher doses also reduced the deposition velocity of iodine onto paint, albeit by a smaller amount than for strategies involving thermal treatments. For all single-strategy ageing tests, the measured deposition velocities remained within a factor of two of the values measured on fresh paint.

Figure 4.3. Adsorption and desorption profiles for AD series tests performed on thermally-cured Amerlock coupons, and for tests performed on pre-irradiated and thermally-cured Amerlock coupons.

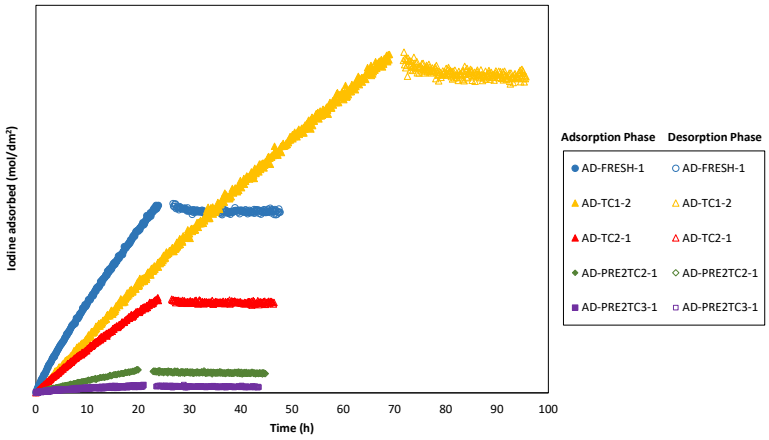

Source: CNL, 2020.
Note: The profile for a freshly painted coupon is also shown for comparison. Loading was performed at 70 °C and 70% relative humidity with an I_2 loading concentration of 1×10^{-8} M.

Consistent with previous BIP studies, very little iodine desorption was typically observed for all single-strategy ageing tests, although combined ageing tests showed relatively higher fractions of iodine to be desorbed. Because very low deposition rates were also observed in these tests, this behaviour suggests that the surface modifications arising from combined ageing strategies (e.g. hydrolysis reactions, cleavage of functional groups, surface annealing) are sufficient to lead to a significant reduction in the number of active sites for iodine adsorption onto paint. As a result, iodine is not strongly retained on the paint surface, and the iodine-paint interaction is likely associated to a greater extent with physisorption.

The explanation that ageing-induced surface modifications are reducing the number of available active sites for iodine chemisorption is supported by leaching tests that were performed on aged Amerlock paint samples in 65°C water. Because of variations in paint thickness, correlations regarding measurements of total organic carbon (TOC) for naturally-aged coupons could not be made with confidence. However, coupons that were aged using pre-irradiations or thermal treatments showed increased TOC releases into water compared to fresh coupons, suggesting that these ageing mechanisms lead to break down of components of the paint structure. Pre-irradiations to higher doses, and the addition of steam during thermal treatments further increased the TOC, indicating that surface modifications have occurred to a greater extent for these samples.

In consultation with the PRG, additional tests with other containment paints were performed to determine if similar ageing trends would be observed. Although the pre-irradiation of Ripolin coupons up to 1 000 kGy did not appear to have any influence on iodine deposition velocity, increased natural ageing of Epigrip coupons led to a decrease in measured deposition velocity, consistent with the Amerlock observations. A small inventory of Gehopon coupons from BIP-2 was also available for testing. The A0 and A30 coupons were originally prepared from the same batch; however, the A0 coupons remained untreated, while the A30 coupons were subjected to a thermal treatment to simulate 30 years of ageing prior to their shipment to the CNL. Figure 4.4 shows the trend in measured deposition velocity at 80°C as a function of relative humidity for Gehopon A0 and A30 coupons, along with Amerlock coupons for comparison. The observation

of increased deposition velocity with increased humidity is consistent with past BIP results. From the figure, it is clear that ageing has a significant effect on the deposition velocity of iodine onto Gehopon. The untreated A0 coupons show deposition velocities of a comparable range to fresh Amerlock; however, a considerable reduction in iodine adsorption rate is observed for the A30 coupons that were thermally aged.

Figure 4.4. Deposition velocities for Gehopon A0 (naturally-aged; solid black line) and Gehopon A30 (thermally and naturally-aged; dashed black line) coupons measured as a function of relative humidity at 80°C and 1×10^{-8} M I_2. Deposition velocities for fresh Amerlock (blue solid line) are also shown for comparison

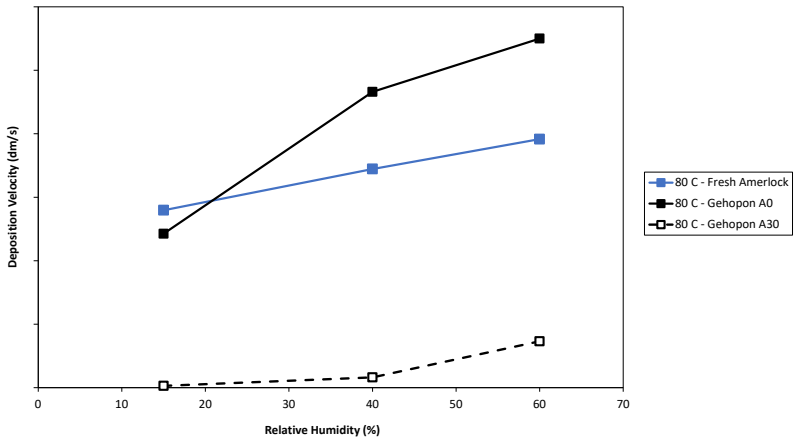

Source: CNL, 2020.

The effect of paint ageing on radiolytic methyl iodide production was also studied in BIP-3. As described in Section 3.3.1, coupon irradiation tests in BIP-3 were performed using two vessel designs. To distinguish between tests in the different vessels in the figures, solid lines have been used for tests performed in the traditional O-ring vessel and dashed lines are used for tests performed in the O-ring free vessel. Methyl iodide production measured during the irradiation of Amerlock coupons aged using pre-irradiation treatments is shown in Figure 4.5. Methyl iodide concentrations measured for fresh Amerlock and a combined ageing strategy test are also shown for comparison. Coupons with increased pre-irradiation dose showed lower methyl iodide production and reached lower steady-state concentrations, regardless of the test vessel used (Figure 4.5). Similar to the iodine sorption tests discussed previously, combined ageing strategy tests showed an additive effect, leading to further reductions in CH_3I production. Comparable trends were observed for naturally-aged and thermally-cured coupons.

The influence of paint ageing on the methyl iodide production can, once again, be explained by surface modifications that are reducing the available chemisorption sites. Although the initial iodine loading for all coupon irradiation tests is nominally the same, a larger fraction of iodine may be physisorbed rather than chemisorbed at active sites on the surface. As a result, these iodine species cannot participate as effectively in chemical reactions with the paint, leading to reductions in methyl iodide production.

Figure 4.5. Summary of methyl iodide concentrations measured as a function of irradiation time for tests with Amerlock coupons aged using pre-irradiation treatments, or the combination of pre-irradiation and heat treatment, in the O-ring (solid lines) and O-ring free (dashed lines) irradiation vessels

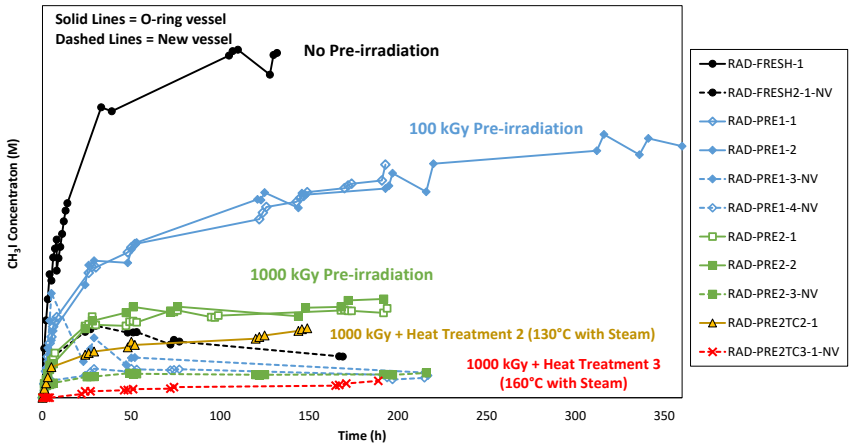

Source: CNL, 2020.

4.3. Pre-exposure to reactive gases

There is an ongoing concern that reactive species in the post-accident containment atmosphere (such as NO_2 and Cl_2) may compete with I_2 for active sites on paint surfaces, which could impact subsequent iodine-paint interactions. Preliminary tests were performed on this topic in BIP-2 and showed a negligible effect; however, the pre-exposure concentrations used were low (5 ppm) and the pre-exposure period may have been too short to see an effect. This topic was further studied in BIP-3 using higher concentrations (up to 1 000 times larger than the subsequent I_2 loading concentration) and longer exposure periods than those used for BIP-2.

Figure 4.6 shows the iodine sorption behaviour onto Amerlock coupons with and without a 4 h pre-exposure to either 245 ppm NO_2 or Cl_2 gas, measured under standard BIP loading conditions (70°C, 70% RH, 1×10^{-8} M I_2). An induction period for iodine adsorption is observed for the pre-exposure tests, whereby the rate of iodine adsorption increases with loading time. This behaviour appears to suggest that NO_2 and Cl_2 can adsorb onto, or react with, the paint during the pre-exposure period and compete with I_2 for adsorption sites upon initiation of the iodine flow. Over time, the reactive species are eventually displaced from the sites, either through thermal desorption or competitive interaction with I_2, and the rate of iodine adsorption is observed to increase. By examination of Figure 4.6, Cl_2 appears to be more competitive than NO_2 for I_2 adsorption sites. Given that Cl_2 is a halogen, similarities to I_2 with respect to its reactivity and affinity for adsorption onto paint are expected.

Figure 4.6. Adsorption and desorption profiles for AD series tests performed on fresh Amerlock coupons with and without a 4 h pre-exposure to either 245 ppm NO_2 or Cl_2 gas. Temperature and humidity were maintained at 70 °C and 70%, respectively, and an I_2 loading concentration of 1×10^{-8} M was used

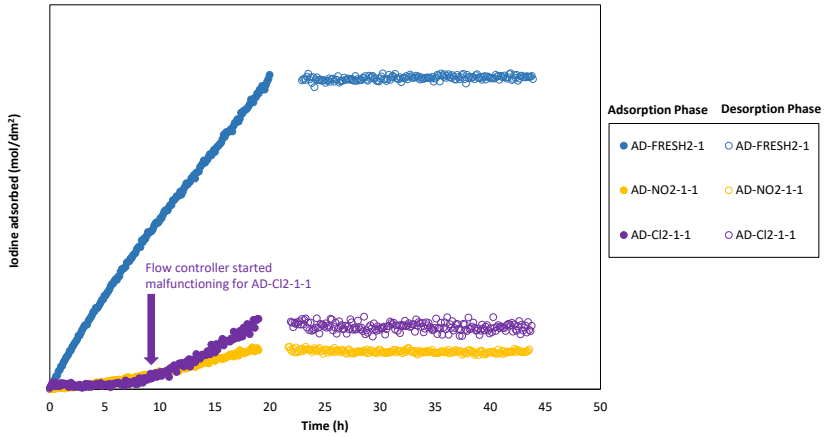

Source: CNL, 2020.

The effect of NO_2 pre-exposures on the subsequent methyl iodide production rate was also evaluated in BIP-3, with results shown in Figure 4.7. In general, while the observed methyl iodide concentrations are slightly lower for paint that has been pre-exposed to NO_2, the pre-exposures appear to have only a small effect on subsequent CH_3I production for coupon irradiation tests.

Figure 4.7. Methyl iodide production as a function of irradiation time for fresh, untreated Amerlock coupons and for coupons pre-exposed to NO_2 gas prior to iodine loading. Tests were performed in the O-ring free irradiation vessel

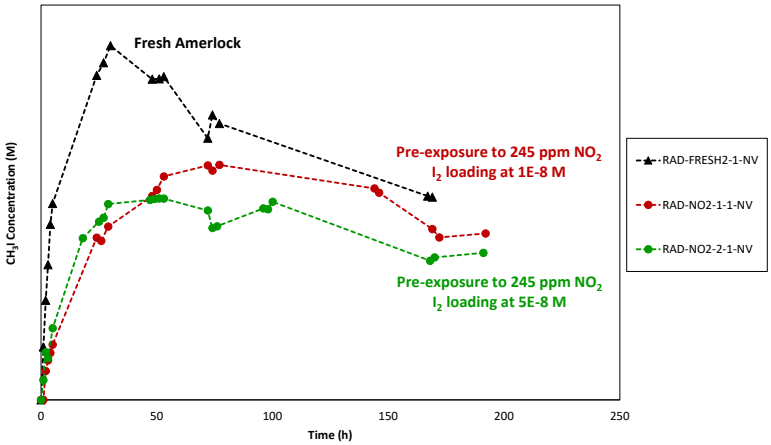

Source: CNL, 2020.

4.4. Effect of water on methyl iodide production

Previous tests in BIP-1 and BIP-2 showed elevated methyl iodide production at the start of an irradiation when the coupons were loaded by submersion in an I_2 solution. This results in a short-term peak in the methyl iodide concentration. Two tests (RAD-AMER-WET-1 and RAD-AMER-WET-2, Figure 3.8) were performed in BIP-3 to conclude investigations of the role of water on methyl iodide production and to simulate the scenario of water condensing onto containment walls after gaseous iodine loading has occurred. Submersion in water after gaseous iodine loading did not result in the same short-term methyl iodide peak that was seen for aqueous loaded tests. The methyl iodide peak observed in BIP-1 and 2 experiments appears to be associated with aqueous adsorption rather than the simple presence of water in the paint matrix, and suggests the nature of the iodine-paint bond is different for gas and aqueous loaded tests.

Figure 4.8. Methyl iodide production measured during irradiation tests of gas-loaded coupons that were submerged in water for 16 hours immediately after loading (red) and after 76 hours of irradiation (blue)

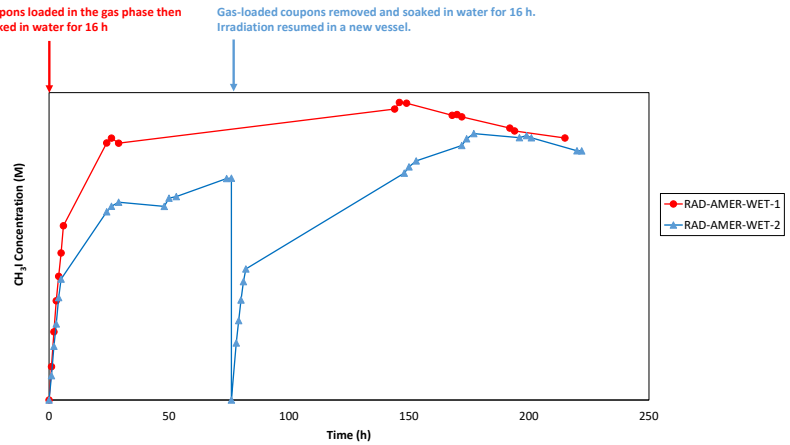

Source: CNL, 2020.

4.5. Iodine interactions with surfaces other than paint

Experiments to evaluate the significance of iodine interactions with surfaces other than paint (glass, O-ring were performed in BIP-3 to assist in the interpretation and modelling of BIP and STEM data and to provide insight into associated experimental uncertainties.

In general, the adsorption of iodine, as I_2 or as CH_3I, onto glass surfaces was shown to be negligible under the conditions studied. However, scoping tests with other solid organic surfaces, such as O-ring material, did show some affinity for the adsorption of these gaseous iodine species.

A selection of irradiation tests were also performed to evaluate the potential for CH_3I release from deposits on glass, or via reaction with other available reactive surfaces (O-ring). Revolatilisation processes were studied as addendums to a limited number of coupon irradiation tests, where the coupons were removed from the vessel, and a second irradiation phase was performed. Iodine revolatilisation was observed in all cases, but for most tests, the CH_3I concentrations measured were somewhat lower than those observed at the conclusion of the prior irradiation phase, and decreased further with time. A redesigned test vessel (Figure 3.10) was used for coupon irradiation tests performed towards the end of BIP-3. A comparison of all

the methyl iodide production profiles that have been measured in BIP-3 (Figure 4.9) for irradiated Amerlock coupons in the traditional O-ring vessel, shown with solid lines, and the redesigned O-ring free vessel, shown with dashed lines, has clearly demonstrated that the presence of other organic materials, even in very small quantities, can contribute to methyl iodide production during the later stages of the irradiation. While differences in the magnitude of CH_3I concentrations are observed between tests performed in the two irradiation vessels, the general trends observed with respect to paint ageing remain consistent.

Figure 4.9. Summary of methyl iodide concentrations measured as a function of irradiation time for all BIP-3 tests performed on Amerlock coupons in the O-ring (solid lines) and O-ring free (dashed lines) irradiation vessels

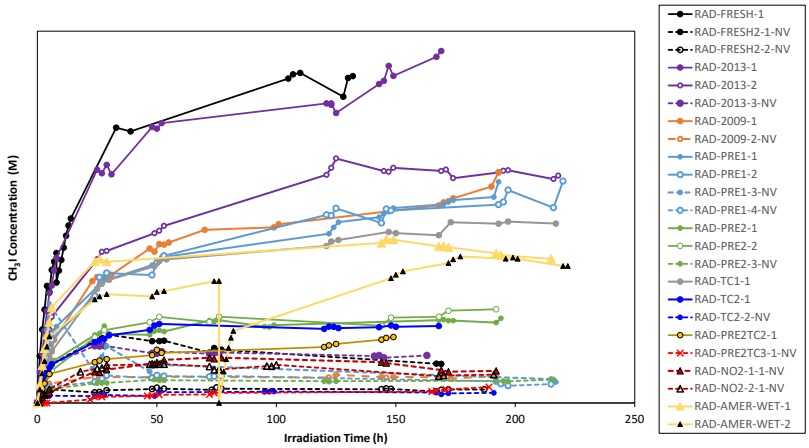

Source: CNL, 2020.

4.6. Gas phase production of methyl iodide

A gas phase reaction between I_2 and volatile organic compounds, such as CH_4, is considered within some iodine behaviour models as a large contributor of methyl iodide in containment (refer to Section 5). The importance of this mechanism, however, is still under debate. The possibility that organic iodides are radiolytically formed to a significant extent in the gas phase is generally dismissed due to the large concentration of O_2 relative to I_2; O_2 is expected to outcompete I_2 for any available $^{\bullet}CH_3$ radicals that are formed. However, some references have suggested methyl iodide production can be significant in such mixtures [6][7].

The CH_4 and CH_3I concentrations measured with time for irradiated mixtures of methane, air (or N_2) and I_2 are shown in Figure 4.10 and Figure 4.11, respectively. Methane is observed to degrade in the radiation field, but the degradation rate was not significantly influenced by the balance gas or the presence of water. Additionally, the methane degradation rate did not noticeably change with increased I_2 concentration, despite the I_2 concentration being varied by more than two orders of magnitude. This suggests that methane removal is proceeding more effectively through reaction with other available species, such as O_2.

Figure 4.10. CH_4 concentrations measured as a function of irradiation time for various CH_4/I_2 gas mixtures

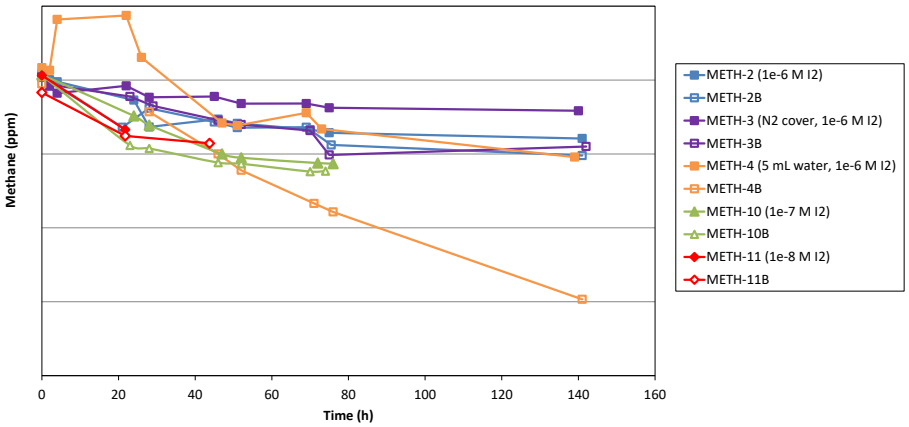

Source: CNL, 2020.

Figure 4.11. CH_3I concentrations measured as a function of time for various CH_4/I_2 gas mixtures. Tests performed with irradiation are shown with solid lines, and tests performed in the absence of radiation are shown with dotted lines

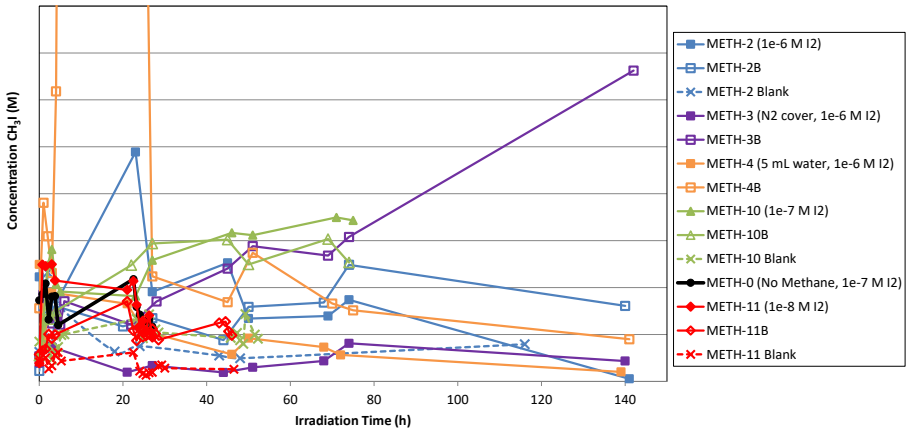

Source: CNL, 2020.

While the experiments appeared to show some conversion to methyl iodide in the radiation field, closer examination of the trends in Figure 4.12 suggests any such conversion is small and difficult to quantify. Increased measurement uncertainties for CH_3I were noted for gas samples with relatively high I_2 concentrations, and an irradiation test performed without methane present yielded comparable CH_3I concentrations to most of the other irradiated CH_4/I_2 mixtures. Ultimately, the contribution of this reaction pathway to CH_3I production for irradiation tests remains unclear, but it does not appear to be a significant contributor compared to the production from painted coupons.

5. Summary of BIP-3 AWG modelling outcomes

Two modelling exercises were performed by the BIP-3 AWG. Six different computational codes were used to model the selected scenarios, ranging from commercially-available severe accident codes to research codes that have been developed and maintained internally by the participating organisations. While some of the codes are semi-empirical in nature and describe phenomenological iodine-paint behaviour, others are significantly more detailed, with larger reaction databases, and use a mechanistic approach to evaluate iodine-paint interactions. Outcomes from the modelling studies will be only summarised. Specific details are provided in the BIP-3 AWG Summary report [8].

The main objective of the Stage 1 exercise was to evaluate how sensitive the simulated predictions of total airborne iodine are towards the inclusion or exclusion of sub-models related to the radiolytic formation of organic iodides from iodine-loaded paint ($ORGI_{PAINT}$)[4] using a simple postulated severe accident scenario.

In general, all models predicted that the inclusion of $ORGI_{PAINT}$ formation would increase the total airborne iodine. Similar trends in predicted iodine behaviour and volatility were also observed with respect to the simulated sump acidification. However, the results also highlighted other areas where significant variations in model capabilities or modelling strategies exist. In particular, there was little consistency among the models in the selection of I_2 deposition velocity, or the treatment of mass transfer. There was also a lack of consensus on which chemical processes were considered, and the outcomes of those processes. Specifically, the gas phase formation of IOx from the radiolysis of I_2 or ORGI, the gas phase reaction of I_2 with volatile organic products to generate ORGI, and the aqueous chemistry of iodine under irradiation at 100 °C were all addressed differently within the different models.

Key observations from the Stage 1 modelling exercise were:

- Despite the range of adsorption rates and mass transfer parameters used in the different models, all models predicted that gaseous I_2 entering the containment is largely adsorbed on the epoxy paint, and can be converted to IOx (rather than be transferred to the sump) when this process is considered.
- The main sources of gaseous ORGI are attributed to the radiolytic reaction of I_2 with the paint surface, and for some models, a gas phase reaction of I_2 with organics. Both of these pathways have been studied in part through the BIP-3 experimental programme. However, the relative importance of the latter mechanism remains unclear.
- Variation of the selected I_2(g) deposition velocity was shown to lead to opposite trends in ORGI concentration in different codes. This deviation highlights how different approaches to modelling ORGI formation, including the iodine phenomenology that is considered (especially in the gas phase), strongly impact model predictions. This suggests some fundamental iodine chemistry pathways should be revisited to ensure that continued model development is based on accurate mechanistic understanding.

4. For simplicity, organic iodides (ORGI) formed radiolytically from painted surfaces with adsorbed iodine are termed $ORGI_{PAINT}$. Codes may include organic iodide production by other means, such as radiolytic formation in the sump ($ORGI_{SUMP}$), radiolytic formation in the gas phase ($ORGI_{GAS}$) and thermal formation in all phases.

The main objective of the Stage 2 exercise was to more critically evaluate predictions from the different iodine-paint interaction models in comparison to available experimental data from two selected benchmark tests: the STEM LD3 test, and the BIP-2 RAD-EPICUR-A1 test.

STEM experiments have shown that organic and inorganic iodine species are quickly released during the first 10 to 15 hours of irradiation and then the release rate decreases significantly for longer irradiation times. BIP-2 experiments have shown that the gaseous organic iodide concentration increases quickly during the first hours of irradiation and reaches a steady state over the long term. The steady state is interpreted to be the result of an equilibrium between organic iodide formation reactions and organic iodide decomposition. The main ORGI formation routes in the gas phase were considered to be release from painted surfaces; however, the BIP-3 AWG modelling efforts and further investigations in the BIP-3 experimental programme have shown that other mechanisms are also likely to have played a role in the tests. Iodine interaction (as both I_2 and ORGI) with the BIP-2 vessel O-ring and the gaseous radiolytic reaction of I_2 with volatile organic compounds are postulated as alternative sources, but there is still no consensus on the importance of each of these mechanisms.

Key findings from the Stage 2 modelling exercise were as follows:

- Although the STEM LD3 test data are generally well modelled by the codes, there is no consensus on the reactions and processes that are considered. From one code to another, I_2 desorption is not always considered in the same way and ORGI release models are very different (e.g. consideration of gaseous reactions between I_2 and volatile organics). The experimental data collected in recent phases of the STEM and BIP projects should help developers refine and validate their iodine-paint interaction models for iodine adsorption and release.
- Modelling results for the CH_3I production in the second irradiation phase of the RAD-EPICUR-A1 test varied widely among codes, and deviated considerably from the measured experimental values, with both overestimation and underestimation of the CH_3I concentrations observed. This suggested that other sinks or sources of CH_3I exist beyond I_2 revolatilisation from IOx deposits on glass followed by adsorption and reaction with the paint surface. Four additional mechanisms were proposed, and are listed below. Each mechanism has been addressed in part through the BIP-3 experimental programme, and recommendations related to these possible mechanistic pathways are considered in Section 7.
    1. Radiolytic gas phase reactions between I_2 and organic compounds released by the paint.
    2. Adsorption/desorption processes involving CH_3I with glass vessel or O-ring surfaces.
    3. Chemical reactions between the paint and deposited IOx on the paint surface.
    4. Chemical reactions between I_2 and/or CH_3I and the rubber O-ring employed to seal the vessel.

It is clear from the observations described above that the nature of the test (batch or on-line), and the uncertainties therein, should be considered in our interpretation of the data. However, the differences in the phenomenology considered among the codes (particularly in the gas phase) can strongly impact model predictions. This indicates that continued refinement of our understanding of fundamental iodine chemistry pathways is needed to ensure continued model development is based on accurate mechanistic behaviour. Furthermore, development efforts should endeavour to limit the potential for user effects to impact on model outcomes.

Specifically, parameter values should be, as much as possible, non-user dependent, and fitting parameters should be independent of the test considered.

6. Overall conclusions

As with its predecessor projects, BIP-3 has continued to expand the available database of iodine deposition data and organic iodide production that can be used towards the development and validation of iodine models. A number of research topics were selected for study to enhance understanding of iodine-paint interactions that may occur in containment, particularly with respect to ageing processes or reactive gas exposure, and to assist in the interpretation of laboratory experiments, including the quantification of uncertainties.

BIP-1 and BIP-2 showed that higher temperatures and relative humidities yield higher rates of iodine adsorption onto paint, with iodine being strongly retained. In BIP-3, exposures using higher iodine loading concentrations were correlated with reduced iodine deposition velocity, and increased relative iodine desorption. This is thought to be associated with a larger fraction of iodine being more loosely-bound, or physisorbed to the paint, under these conditions. As a result, the effectiveness of paint as an iodine sink in containment is somewhat dependent on the conditions of iodine exposure (i.e. I_2 concentration).

Most of the other phenomena studied in BIP-3, including paint ageing and reactive gas pre-exposures, also led to reduced rates of I_2 adsorption onto Amerlock paint. Aside from pre-irradiated Ripolin, the other containment paints studied seemed to demonstrate similar trends in iodine deposition with respect to ageing. These data suggest that aged paint is a less effective iodine sink than fresh paints, and could contribute to increased airborne iodine in containment. However, it appears that nearly all of the iodine adsorption rates measured for different paints and ageing strategies in BIP-3 fall within the range of deposition velocity values that are currently applied in iodine chemistry models, and, aside from combined ageing tests and tests with pre-exposures to reactive gases, the iodine adsorption rates measured for Amerlock coupons spanned only a factor of two.

Coupon irradiation tests performed in BIP-3 showed that methyl iodide production from iodine-loaded paint was generally reduced as a function of age, with the combination of ageing strategies leading to a greater reduction. This implies that, for aged paint, a larger fraction of the volatile iodine in containment may remain as I_2, which is more easily trapped than CH_3I with conventional filtration systems.

The gas phase production of methyl iodide from the irradiation of I_2 and CH_4 gas mixtures was also evaluated in BIP-3. Some iodine behaviour models consider this reaction to be a large contributor of methyl iodide in containment. While low CH_3I concentrations were detected in these irradiation tests, large experimental uncertainties were assigned to the measurements (owing to the high I_2 concentrations). Examination of the data trends appears to suggest that this reaction is not a significant contributor to gaseous CH_3I compared to the production from painted coupons. However, the overall contribution of this reaction pathway to CH_3I production remains unclear.

The production or release of methyl iodide through interactions with other surfaces of the BIP irradiation vessel were also explored in BIP-3. The revolatilisation of iodine from deposits on glass produced detectable concentrations of methyl iodide that decreased with further irradiation time. Additionally, the presence of other organically-based materials, even in very small quantities, were shown to contribute to methyl iodide production in irradiation tests, particularly over the long term. Coupon irradiation tests performed in a redesigned vessel that minimised uncertainties associated with organically-based seals yielded lower methyl iodide concentrations than comparable tests in the previous vessel, although general trends with respect

to paint ageing remained consistent among the two vessels. This observation may also help to rationalise some of the deviations observed between model simulations and BIP-2 experimental data through the AWG.

It should be noted that the organic iodide production rates from the irradiation of iodine-loaded paint measured in BIP-1 and BIP-2 are among the lowest in the available literature [4], and concentrations observed from recent BIP-3 tests are lower still. In part this can be attributed to the fact that BIP measures methyl iodide as a surrogate for all organic iodides. While the recent BIP-3 coupon irradiation tests may be considered optimised for separate effects testing of iodine-paint interactions, other solid organics will be present in containment (such as cable coatings). The interaction of iodine with these materials, and how these interactions may contribute to the iodine source term, is not necessarily well understood. In the context of model development, some consideration should be given to the level of conservatism appropriate for such methyl iodide production mechanisms.

7. Recommendations

The BIP-3 programme has demonstrated that paint ageing can have a significant effect on iodine sorption and organic iodide production. The overall consequences of this phenomenon on predictions of iodine speciation and volatility should be assessed in full scale accident analyses.

The relative importance of radiolytic gas phase reactions between I_2 and volatile organic compounds on methyl iodide production remains unclear. Resolution will require additional tests with an improved analytical method.

The presence of other organically-based materials was shown to contribute in part to the long-term methyl iodide production for coupon irradiation tests in BIP-3. Tests to assess the organic iodide production that may arise from organics in containment other than paint (e.g. cable coatings) could be considered to assist in future model development and to better quantify predictions of iodine source term.

The redesigned BIP-3 irradiation vessel minimised uncertainties associated with organically-based seals and was better able to isolate the methyl iodide production arising from iodine-paint interactions. A future modelling exercise could be considered using a benchmark test performed in this vessel.

In general, the AWG modelling exercises revealed that differences in the phenomenology considered among the codes (particularly in the gas phase) can strongly impact model predictions. This indicates that continued refinement of our understanding of fundamental iodine chemistry pathways is needed to ensure continued model development is based on accurate mechanistic behaviour. Additionally, continued model development efforts should endeavour to limit the potential for user effects to impact on model outcomes, and wherever possible, fitting parameters should be independent of the test considered.

8. References

[1] NEA (2007), *State of the Art Report on Iodine Chemistry,* NEA/CSNI/R(2007)1, OECD Publishing, Paris, www.oecd-nea.org/jcms/pl_18434.

[2] NEA (2012), *OECD/NEA Behaviour of Iodine Project: Final Summary Report,* NEA/CSNI/R(2011)11, OECD Publishing, Paris, www.oecd-nea.org/jcms/pl_19098.

[3] NEA (2016), *The Main Outcomes of the OECD Behaviour of Iodine Project*, in "Proceedings of the OECD-NEA International Iodine Workshop, 30 March 30 to 1 April 2015*,* Marseille, France", NEA/CSNI/R(2016)5, OECD Publishing, Paris, pp. 153-164, www.oecd-nea.org/jcms/pl_19702.

[4] Bosland, L. et al. (2014), "Iodine-paint interactions during nuclear reactor severe accidents"*, Ann. Nucl. Energy,* 74, 184.

[5] NEA (2016), *The Behaviour of Iodine Project: A Proposal for BIP-3, in "*Proceedings of the OECD-NEA International Iodine Workshop, March 30 to April 1, 2015, Marseille, France", NEA/CSNI/R(2016)5, OECD Publishing, Paris, pp. 165-171, www.oecd-nea.org/jcms/pl_19702.

[6] Bartoníček, B. and A. Habersbergerová (1986), "Investigation of the Formation Possibilities of Alkyl Iodides", *Nuclear Power Plants. Radiat. Phys. Chem.,* 28(5), 591.

[7] Bartoníček, B. and A. Habersbergerová (1987), *Formation of Methyl Iodide by Ionizing Radiation. Proc. of the 4th Working Meeting on Radiation Interactions,* Leipzig, Germany,
p. 49.

[8] Yakabuskie, P.A., G.A. Glowa and L. Bosland (2020), *Behaviour of Iodine Project 3: Outcomes of the Analytical Working Group. Canadian Nuclear Laboratories R&D Report,* Canadian Nuclear Laboratories, 153-126530-440-023.

[9] Fillet, S. et al. (2012), *LD1, LD2, LD3 STEM/EPICUR tests report – Formation and release of volatile species from painted coupons, IRSN Report,* Institut de Radioprotection et de Sûreté Nucléaire, IRSN-SAG-SEREX 2012-057 STEM nº6.

[10] Glowa, G.A. et al. (2014), *Behaviour of Iodine Project 2: Final Report,* Atomic Energy of Canada Limited Report, 153-126530-440-019.

[11] AFNOR (1996), *Peintures pour l'industrie nucléaire: essai de tenue à des conditions accidentelles de référence (réacteur à eau sous pression) et de réparabilité,* Association Française de Normalisation, AFNOR NF T30–900, ISSN 0335–3931.

[12] ASTM (2008), *Standard test method for evaluating coatings used in light-water nuclear power plants at simulated design basis accident (DBA) conditions,* American Society for Testing and Materials International, ASTM-D3911-08.

[13] Yakabuskie, P.A. et al. (2017), *Behaviour of Iodine Project 3: Year 1 Report,* Canadian Nuclear Laboratories R&D Report.

[14] Glowa, G.A. et al. (2011), *Behaviour of Iodine Project: Final Report on Iodine Adsorption Studies,* Atomic Energy of Canada Limited Report*,* 153-126530-440-013.

[15] Yakabuskie, P.A., G.A. Glowa and D. Boulianne (2018), *Behaviour of Iodine Project 3: Year 2 Report,* Canadian Nuclear Laboratories R&D Report, 153-126530-440-021.

[16] Yakabuskie, P.A., D. Boulianne and J. Nakamura (2020), *Behaviour of Iodine Project 3: Year 3 Report,* Canadian Nuclear Laboratories R&D Report, 153-126530-440-022.